

Impact of evolving radio galaxies on their environment

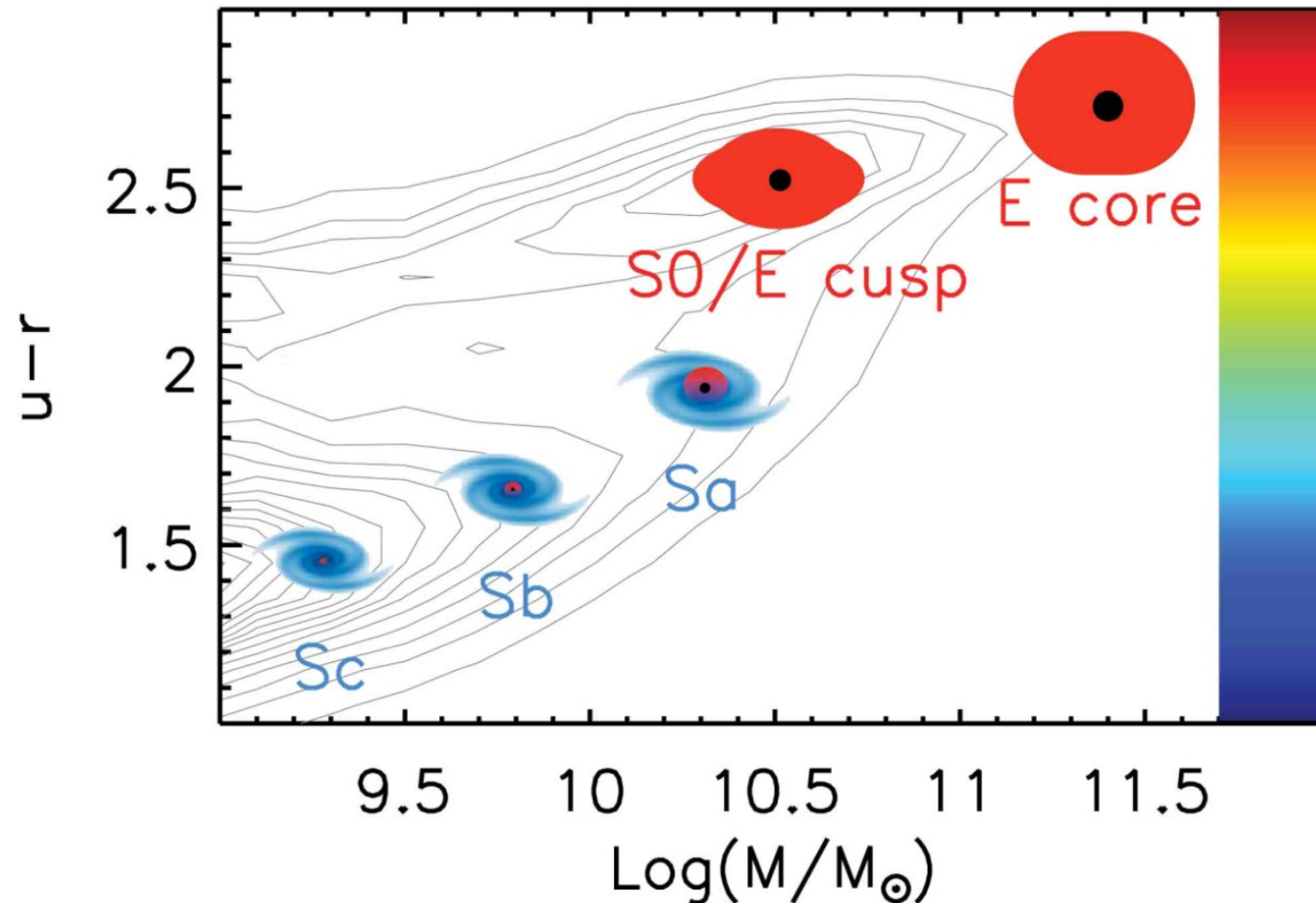
- from the interstellar medium
to galaxy groups and clusters

Łukasz Stawarz

Astronomical Observatory, Jagiellonian University (Kraków, Poland)

July 2018

The galaxy bimodality



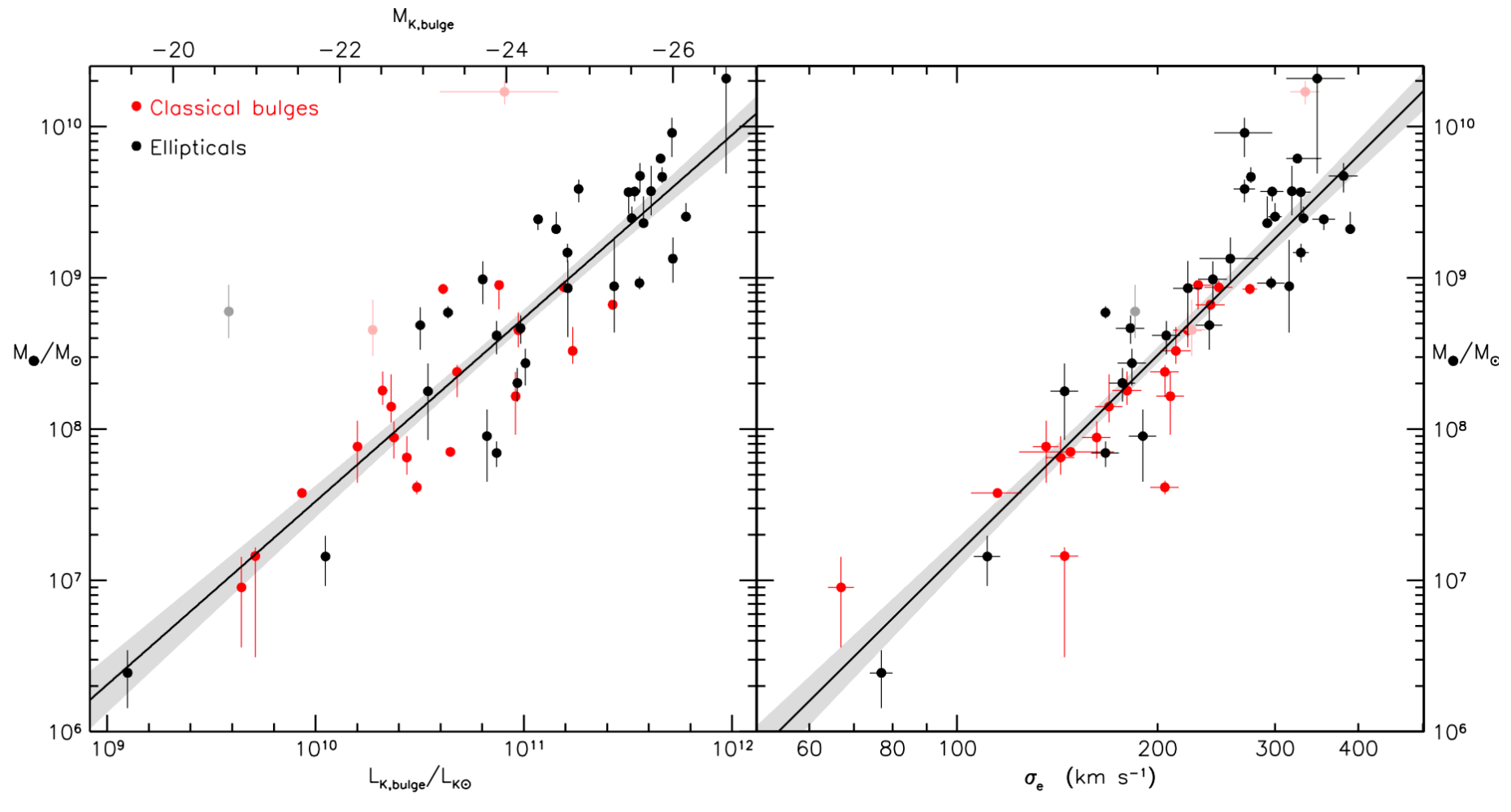
The contours show the galaxy distribution on a stellar mass. Galaxies are classified into two main types: spirals that mainly grew through gas accretion and ellipticals that mainly grew through mergers with other galaxies. All ellipticals and bulges within spirals contain a central black hole.

Cattaneo et al. 2009:

In mergers of galaxies that are still accreting gas, the gas falls to the centre, triggers starbursts, and is often observed to feed the rapid growth of black holes. Black holes respond to this fuelling by feeding energy back to the surrounding gas. This energy produces winds and jets, which may accelerate the star formation rate by compressing the gas. In the most dramatic scenario, all the gas is blown away, so black hole growth and star formation suddenly terminate.

This “quenching” is necessary to explain why ellipticals are red.

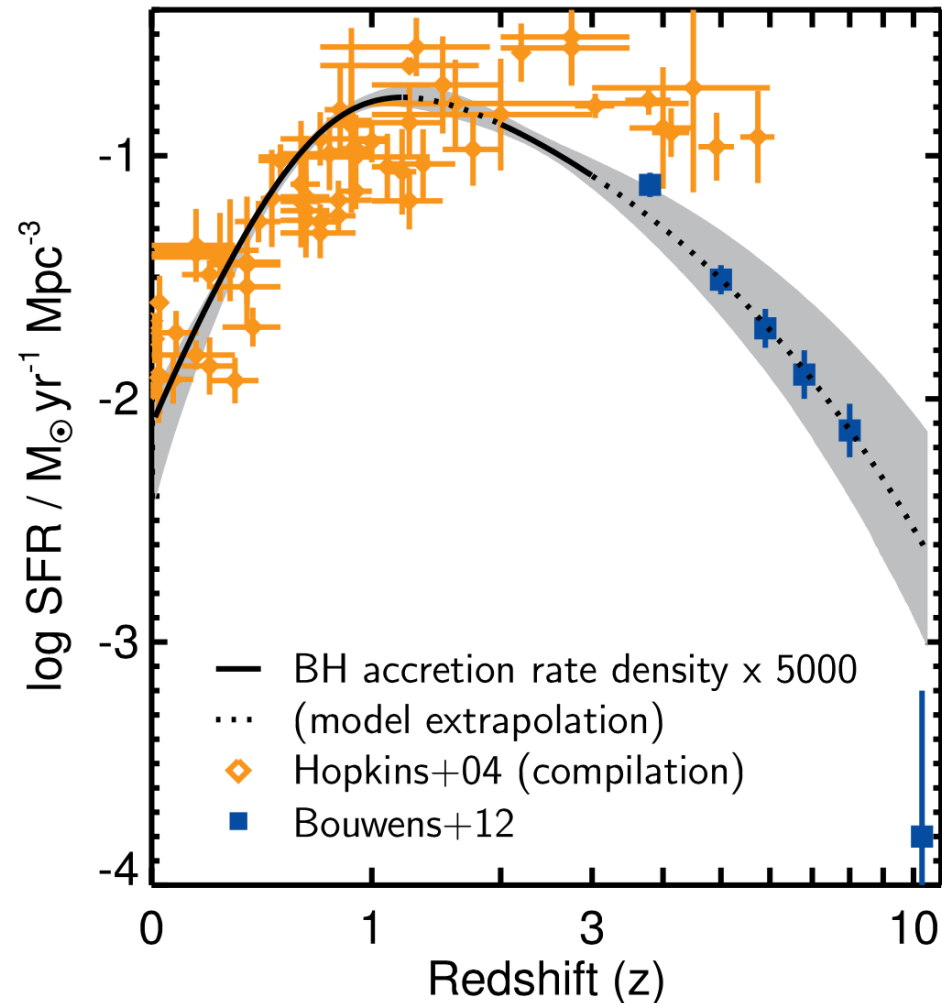
Co-evolution of SMBHs & galaxies



Kormendy & Ho 2013, ARA&A:

The tightness of the M_{BH} correlations with bulge velocity dispersion, etc., suggests that SMBH growth and galaxy formation are connected.

Co-evolution of SMBHs & galaxies



Kormendy & Ho 2013, ARA&A:

The histories of BH growth and star formation in the universe are similar. Quasars and starbursts appear, at least superficially, to be closely linked. The most luminous starbursts always show signs of buried AGNs, even if these do not dominate the bolometric output, and the host galaxies of AGNs often show concurrent or recent star formation.

Co-evolution of SMBHs & galaxies

De Zotti (Proceedings of the 3rd Cosmology School in Cracow 2017):

- The physical scale of the AGNs is incomparably smaller than that of galaxies: typical radii of the stellar distribution of galaxies are of several kpc, to be compared with the Schwarzschild radius

$$r_S = \frac{2G M_{\text{BH}}}{c^2} \simeq 9.56 \times 10^{-6} \frac{M_{\text{BH}}}{10^8 M_{\odot}} \text{ pc},$$

i.e. $r_{\text{BH}} \sim 10^{-9} r_{\text{gal}}$.

- The radius of the "sphere of influence" of the SMBH (the distance at which its potential significantly affects the motion of the stars or of the interstellar medium) is also small:

$$r_{\text{inf}} = \frac{G M_{\text{BH}}}{\sigma_{\star}^2} \simeq 11 \frac{M_{\text{BH}}}{10^8 M_{\odot}} \left(\frac{\sigma_{\star}}{200 \text{ km s}^{-1}} \right)^{-2} \text{ pc},$$

σ_{\star} being the velocity dispersion of stars in the host galaxies (SMBHs are generally associated to spheroidal components of galaxies, whose stellar dynamics is dominated by random motions, not by rotation). Hence SMBHs have a negligible impact on the global stellar and interstellar medium (ISM) dynamics.

Co-evolution of SMBHs & galaxies

De Zotti (Proceedings of the 3rd Cosmology School in Cracow 2017):

As we have seen, the smallness of the radius of influence means that the SMBH's gravity has a completely negligible effect on its host galaxy. On the other hand, the energy released by the AGN

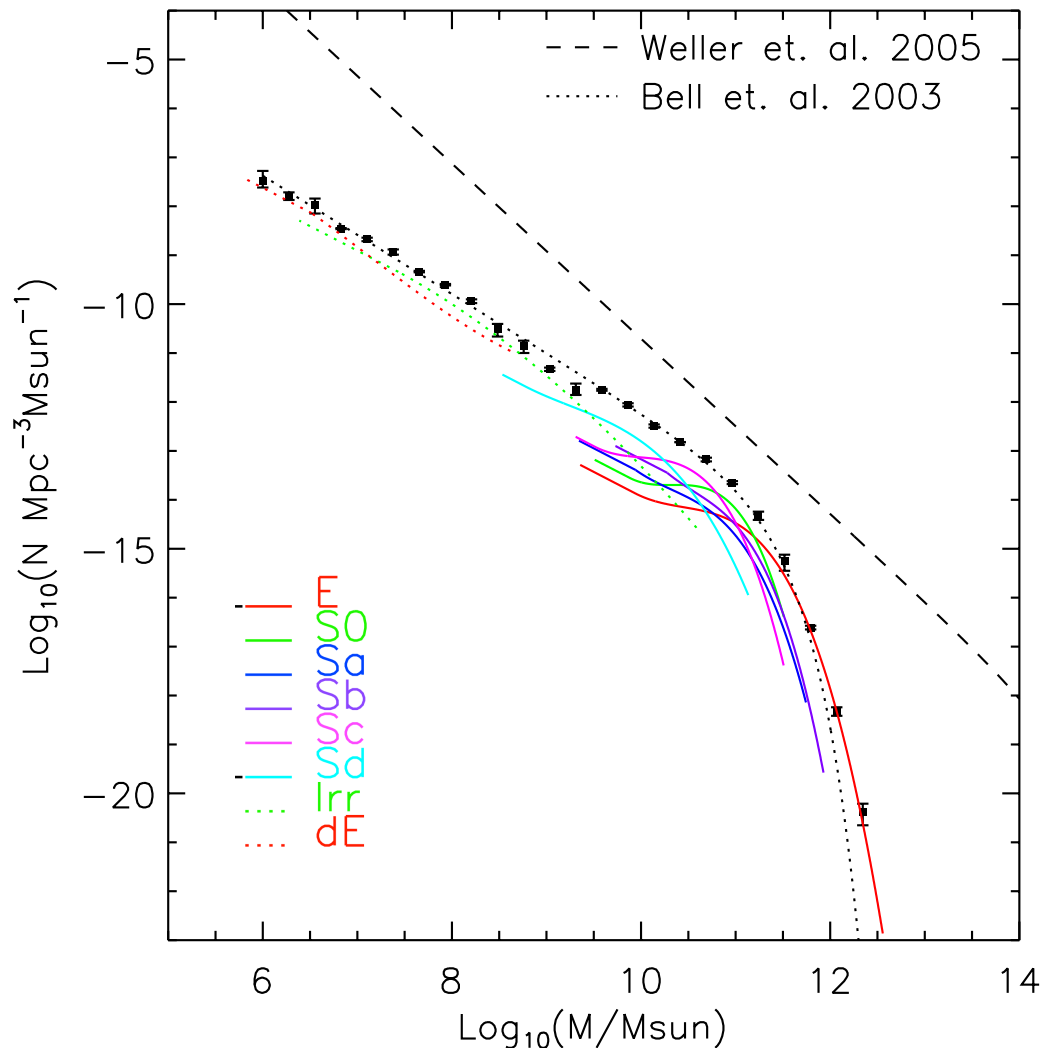
$$E_{\text{BH}} \simeq \epsilon M c^2 \sim 2 \times 10^{61} \frac{\epsilon}{0.1} \frac{M_{\text{BH}}}{10^8 M_{\odot}} \text{ erg},$$

where ϵ is the mass to radiation conversion efficiency, is far larger than the gas binding energy. Setting $M_{\text{gas}} = f M_{\text{bulge}}$, with $f < 1$, we have

$$E_{\text{gas}} \sim \frac{3}{2} f M_{\text{bulge}} \sigma^2 \sim 1.2 \times 10^{58} f \frac{M_{\text{bulge}}/M_{\text{BH}}}{10^3} \frac{M_{\text{BH}}}{10^8 M_{\odot}} \left(\frac{\sigma}{200 \text{ km/s}} \right)^{-2} \text{ erg},$$

where σ is the line-of-sight velocity dispersion (the corresponding 3D velocity is $v = \sqrt{3}\sigma$). This means that only a few percent of the SMBH energy output may have a strong influence on the gas in the host galaxy, potentially expelling it and, at the same time, limiting the SMBH own growth.

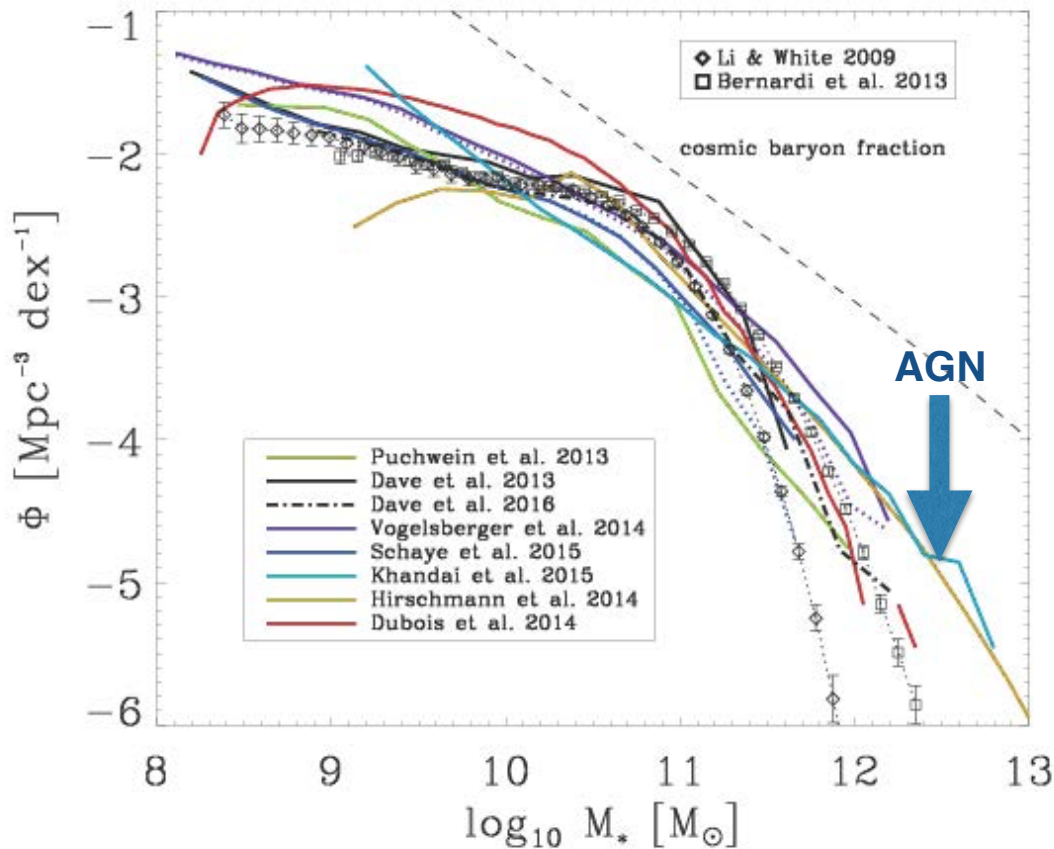
Co-evolution of SMBHs & galaxies



Naab & Ostriker 2017, ARA&A:

The field galaxy baryonic mass function. The data points are for all galaxies, while the lines show spine fits by Hubble Type. The CDM mass spectrum from the numerical simulations is also shown by dashed line [*“the hypothetical galaxy mass function assuming the cosmic baryon fraction”*]. The closer the stellar mass function is to this line, the more efficient star formation is in haloes of the corresponding mass. (...) The differing slopes at both high and low masses indicates that star formation (as a function of halo mass) is less efficient in these regimes.

Co-evolution of SMBHs & galaxies



Naab & Ostriker 2017, ARA&A:

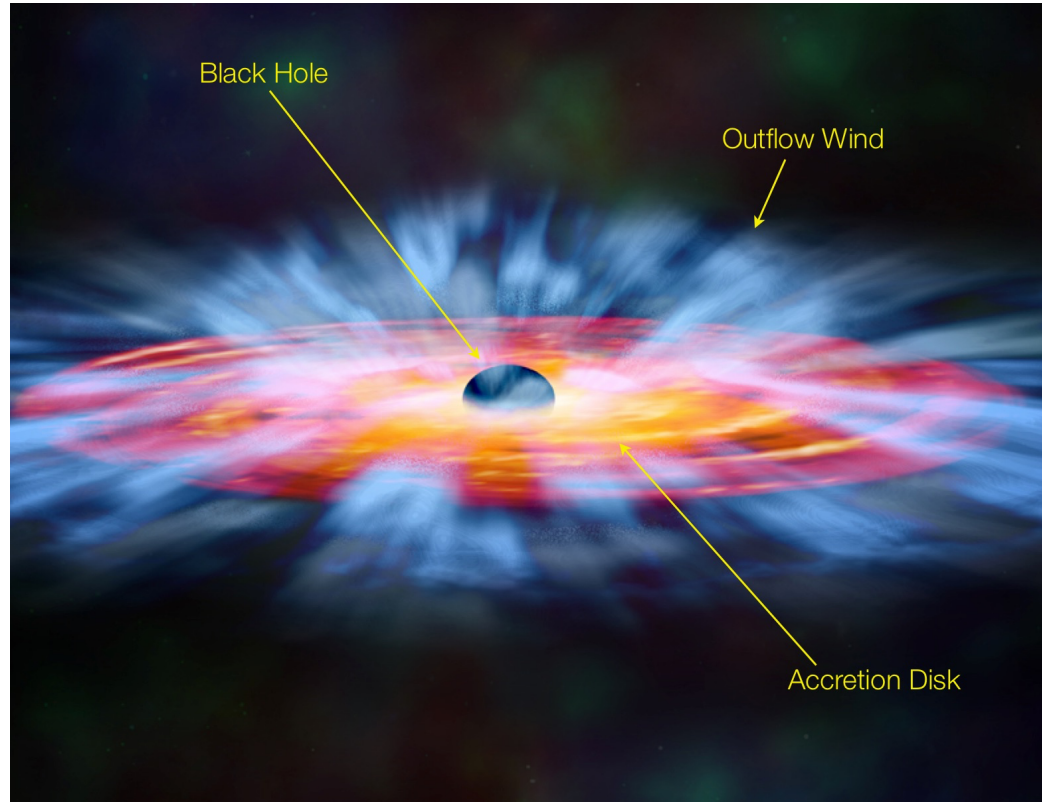
The field galaxy baryonic mass function. The data points are for all galaxies, while the lines show spine fits by Hubble Type. The CDM mass spectrum from the numerical simulations is also shown by dashed line [*“the hypothetical galaxy mass function assuming the cosmic baryon fraction”*]. The closer the stellar mass function is to this line, the more efficient star formation is in haloes of the corresponding mass. (...) The differing slopes at both high and low masses indicates that star formation (as a function of halo mass) is less efficient in these regimes.

At low masses, this is commonly attributed to efficient gas ejection due to supernova feedback, whereas at high masses energy injection from central SMBHs is thought to be able to effectively reduce the efficiency of gas cooling.

AGN “feedback”

- AGN have now become a fundamental component of semi-analytic models and hydrodynamic simulations of galaxy evolution in order to explain the properties of galaxies hosted by massive dark matter haloes ($10^{12} M_{\odot}$). In the absence of AGN feedback, models predict galaxies which are too bright, too compact, too massive and too blue at $z = 0$, compared to the observations.
- **Still, the models discussed so far rely only on some approximate “prescriptions” for the AGN feedback...**
- So how does the feedback operate? What are the observational evidence for the AGN feedback in action?

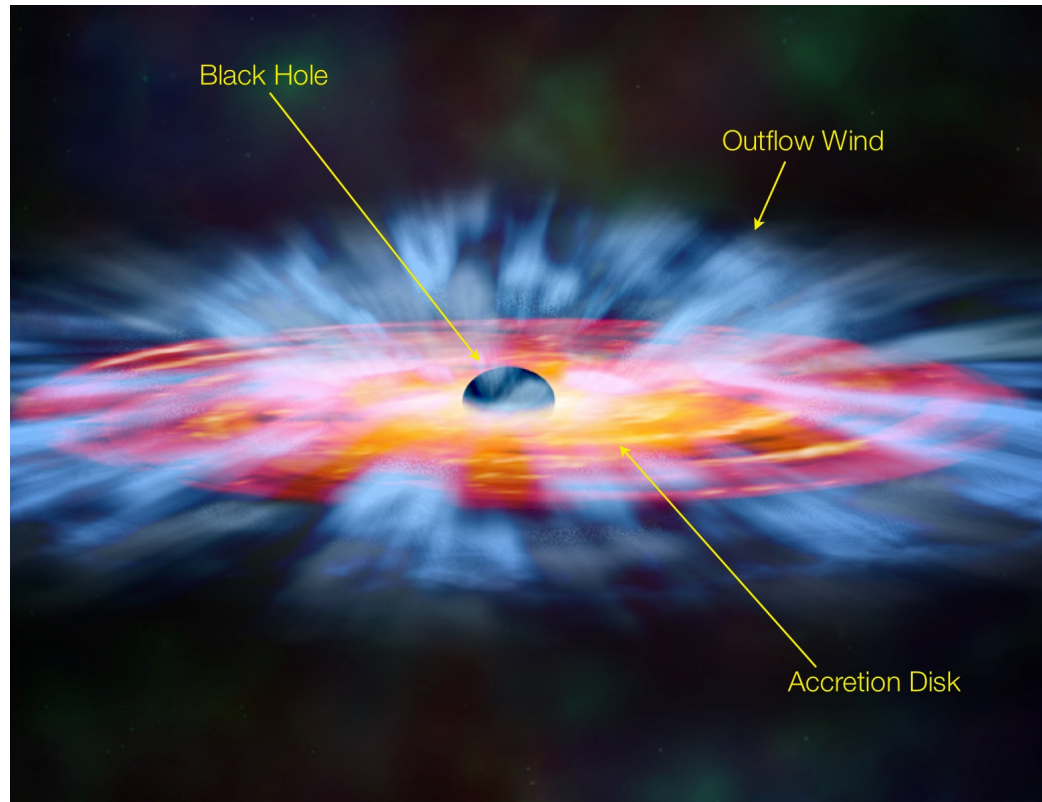
AGN outflows



disk outflows

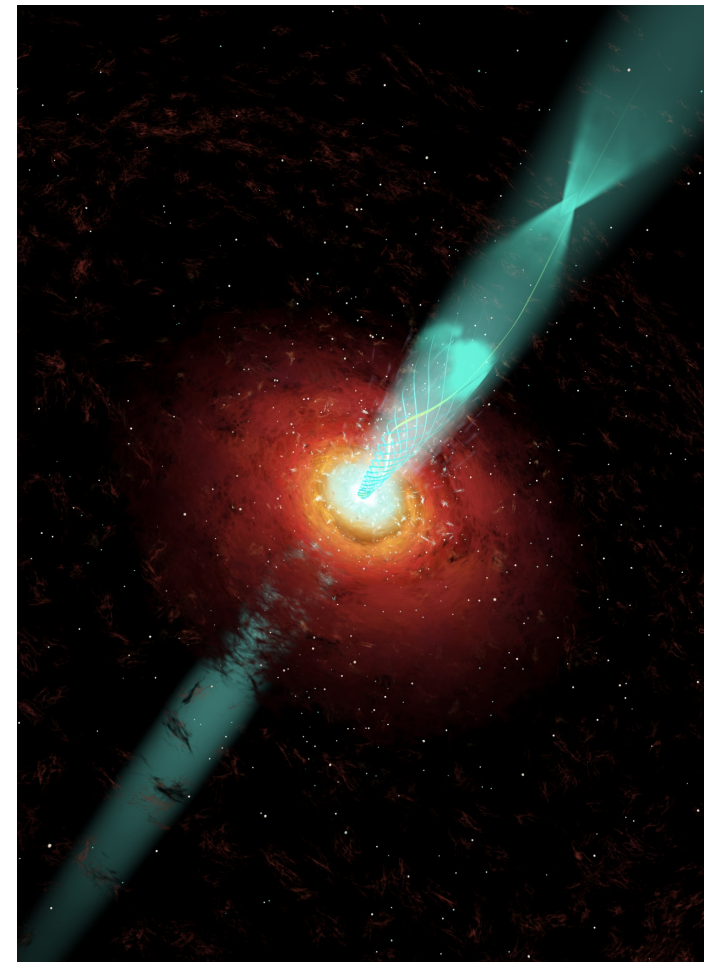
radiation pressure-driven
or magnetically-driven

AGN outflows & jets



disk outflows

radiation pressure-driven
or magnetically-driven

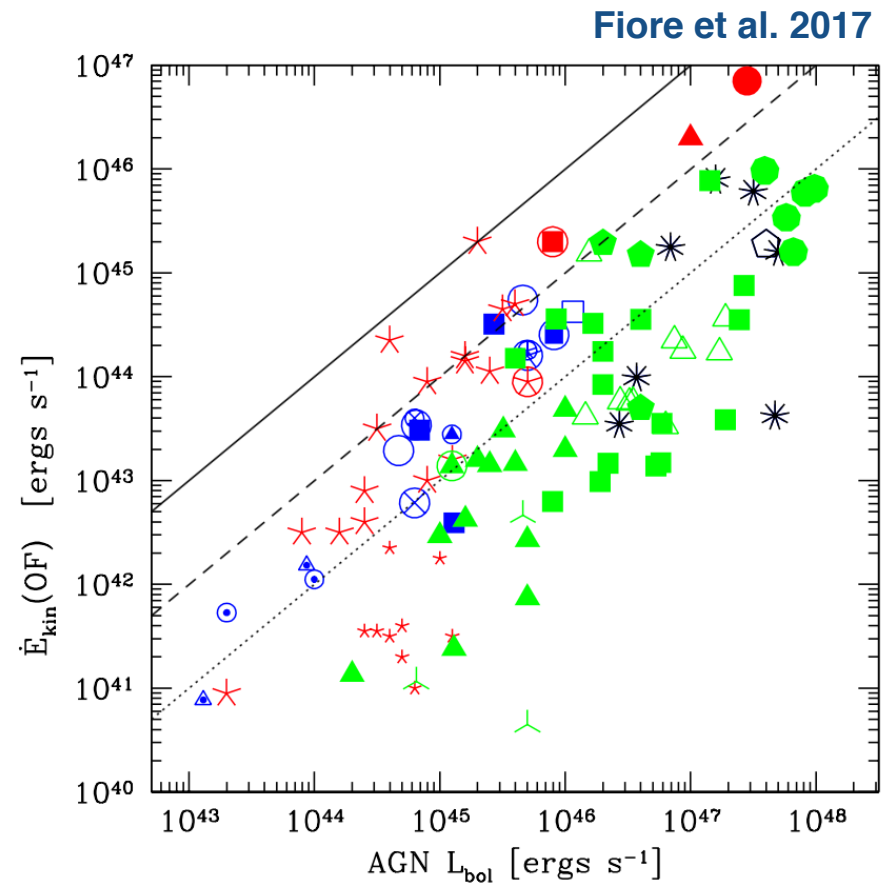
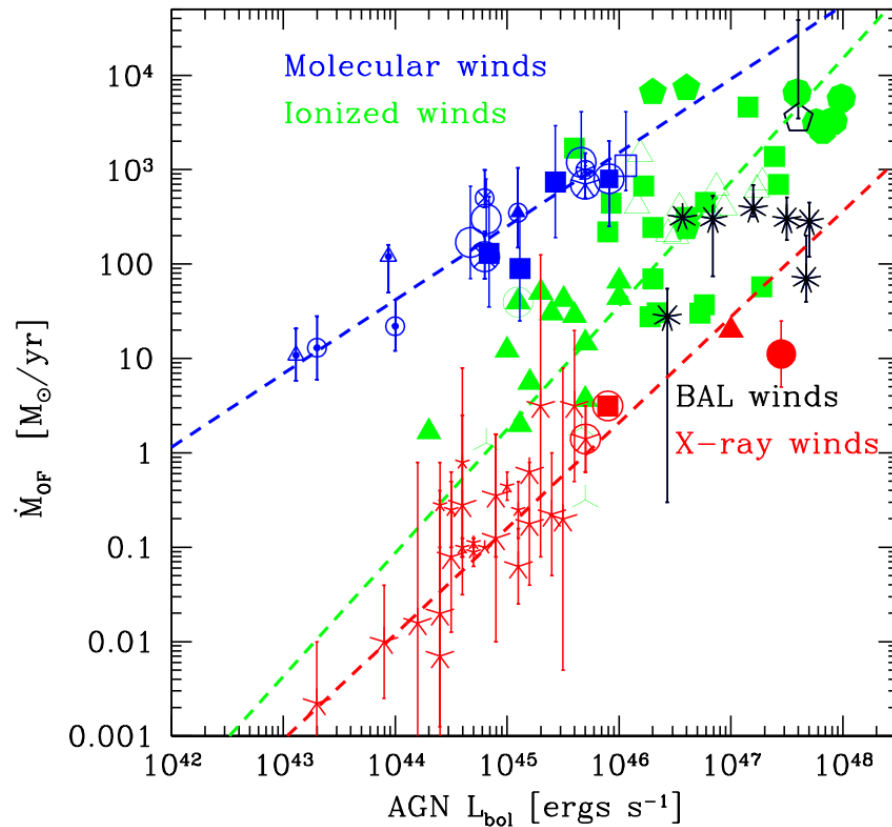


relativistic jets

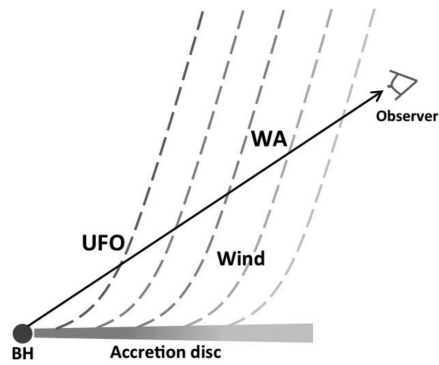
electromagnetic extraction of rotational energy
from disc-fed supermassive black holes

AGN outflows

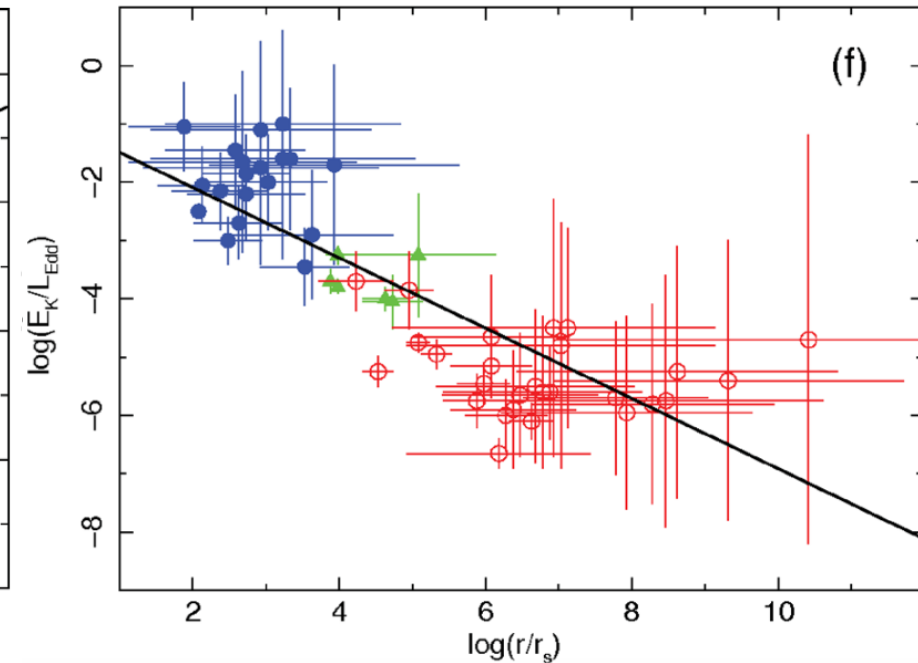
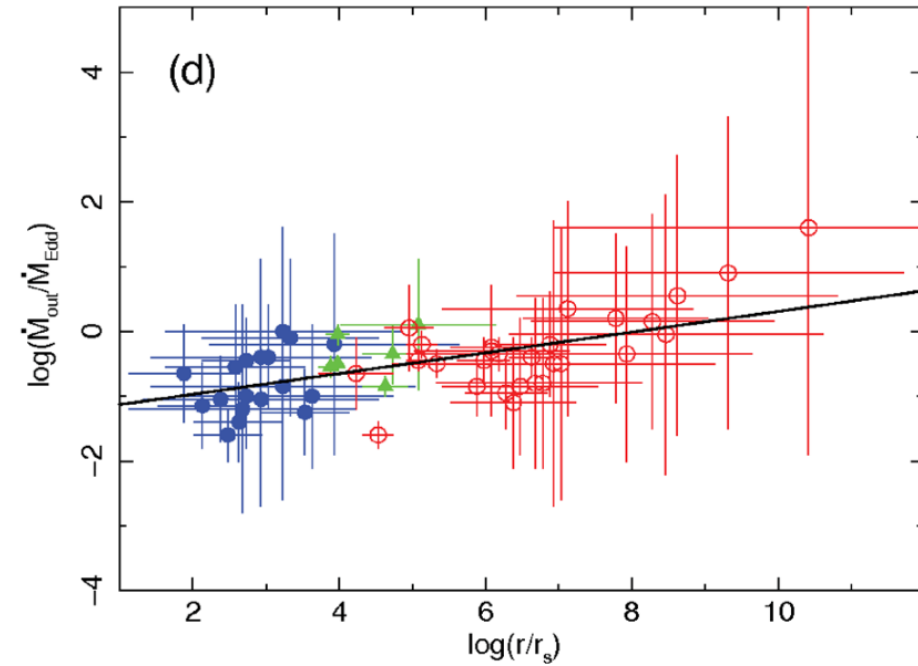
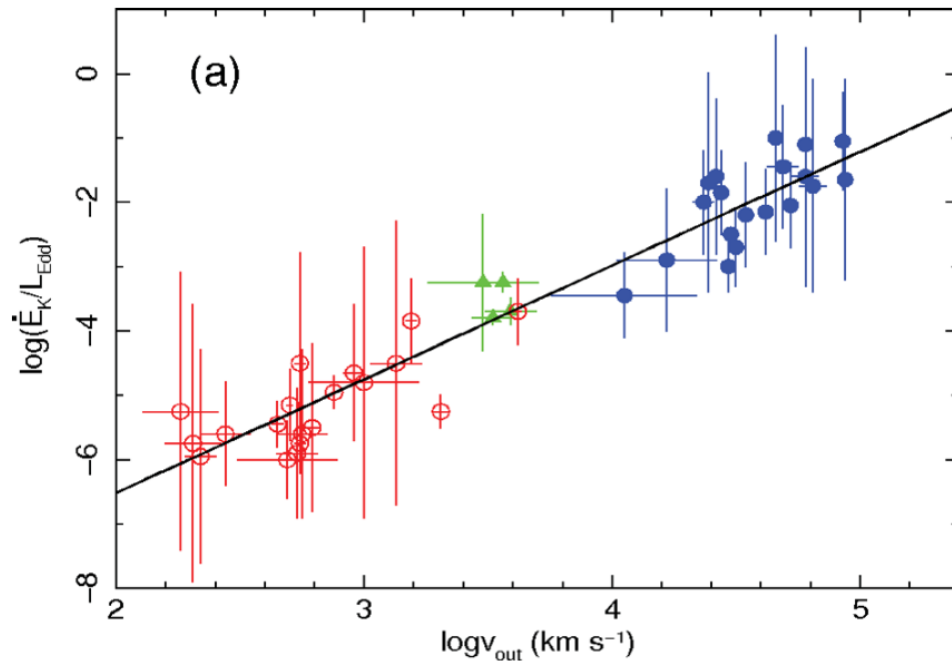
- cold molecular outflows ($T \approx 10$ K) as traced by carbon monoxide (CO) emission lines
- warm ionised outflows ($T \approx 10^4$ K) traced with rest-frame optical or near-infrared emission lines
- warm absorbers observable in absorption in the soft X-rays; ultra-fast outflows (UFOs) traced with highly blue-shifted and highly ionized Fe K-shell absorption lines at ~ 7 keV



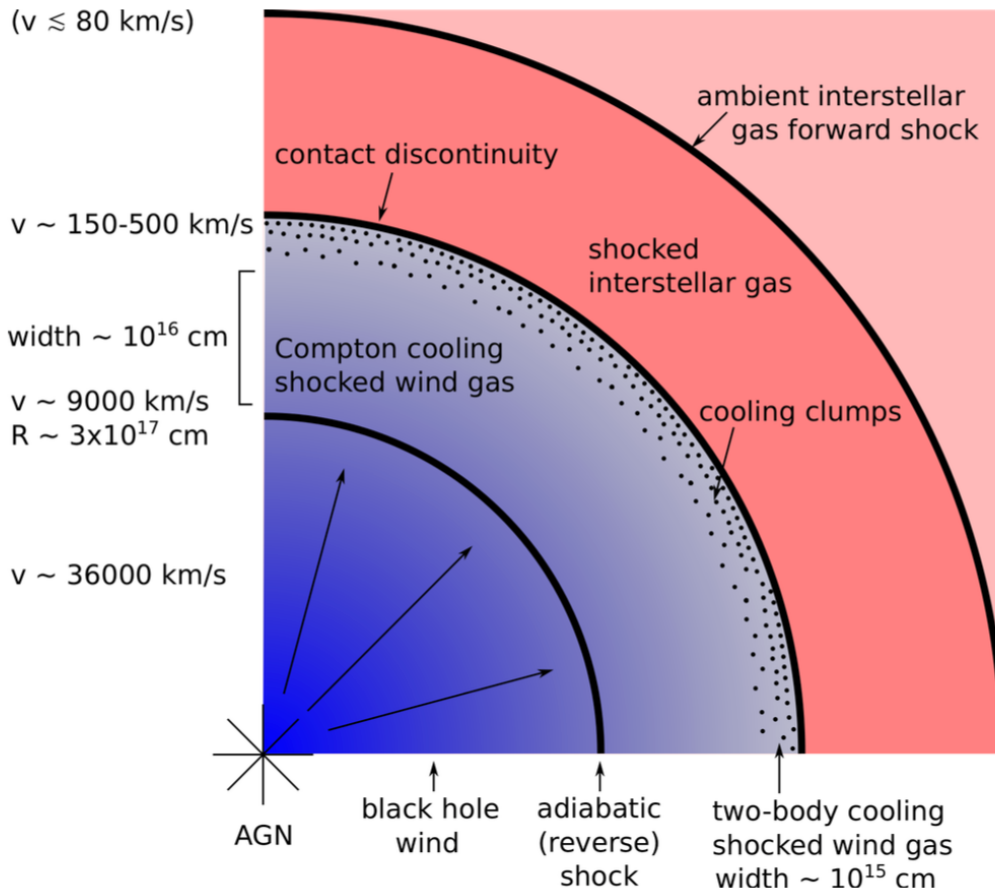
AGN outflows: UFOs



Tombesi et al. 2013



“Radiative Feedback”



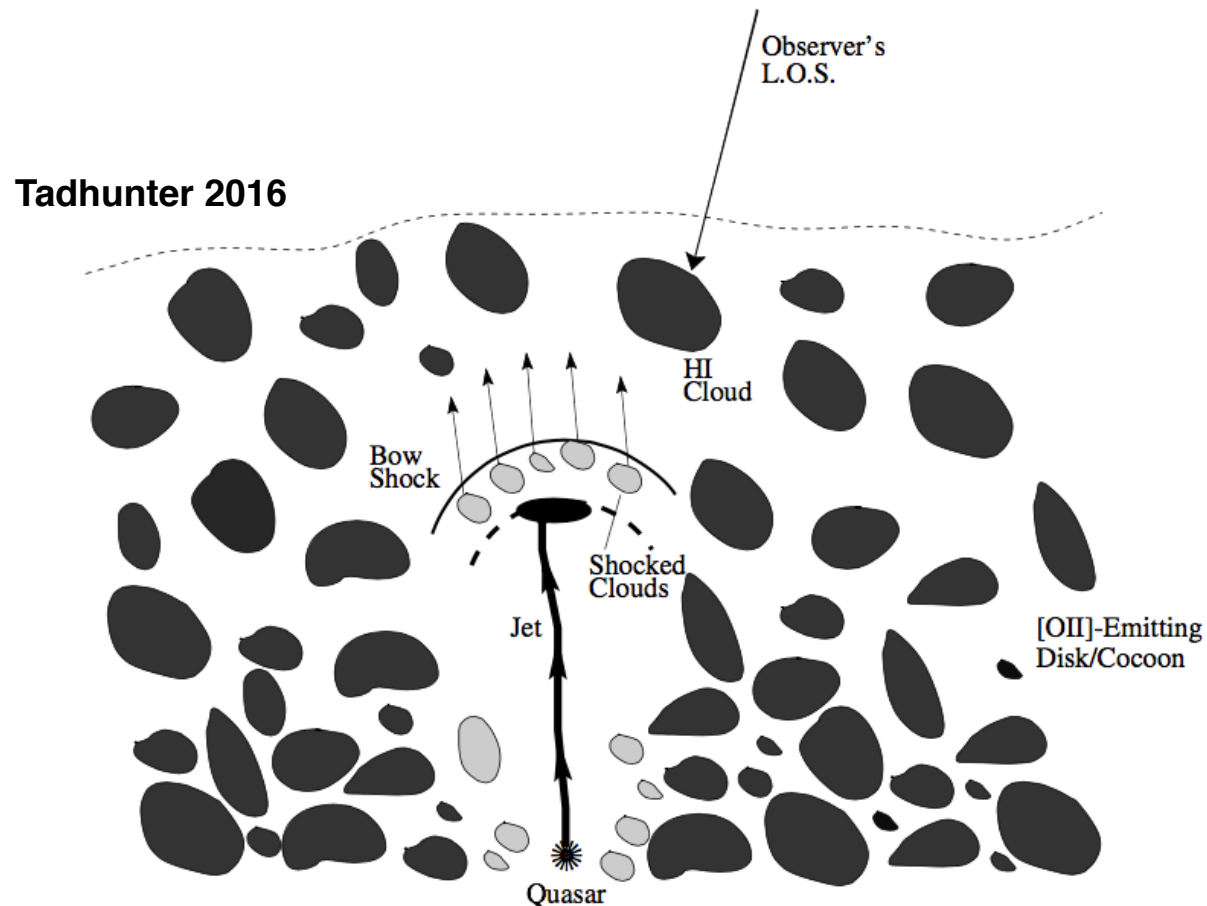
King & Pound 2015:

Schematic view of the shock pattern resulting from the impact of a black hole wind (blue) on the interstellar gas (red) of the host galaxy. The accreting supermassive black hole drives a fast wind (velocity $v \sim 0.1c$). It collides with the ambient gas in the host galaxy and is slowed in a strong shock. The inverse Compton effect from the quasar’s radiation field rapidly cools the shocked gas, removing its thermal energy and strongly compressing and slowing it over a very narrow radial extent. In the most compressed gas, two-body cooling becomes important, and the flow rapidly cools and slows over an even narrower region. The cooled gas exerts the preshock ram pressure on the galaxy’s interstellar gas and sweeps it up into a dense shell (‘snowplow’). The shell’s motion then drives a milder outward shock into the ambient interstellar medium.

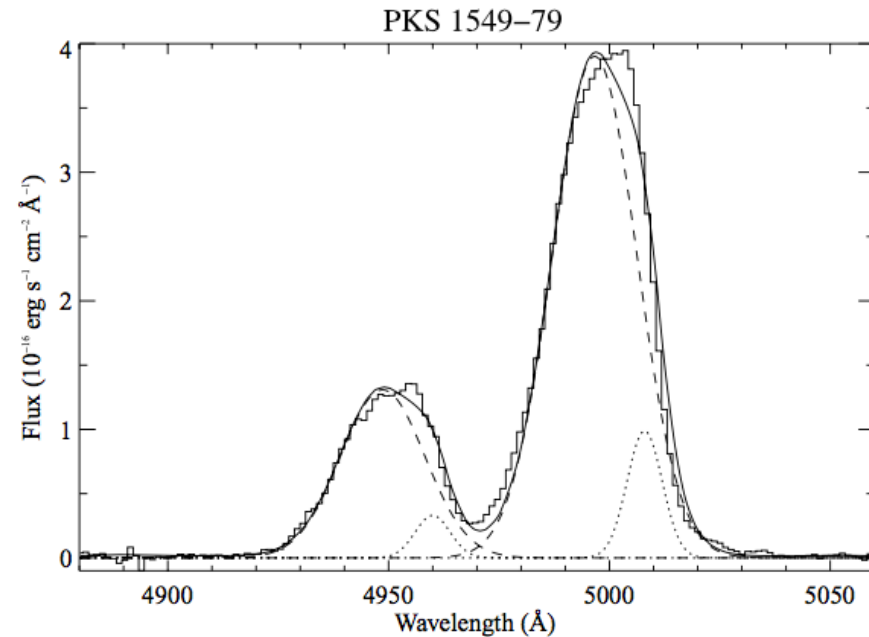
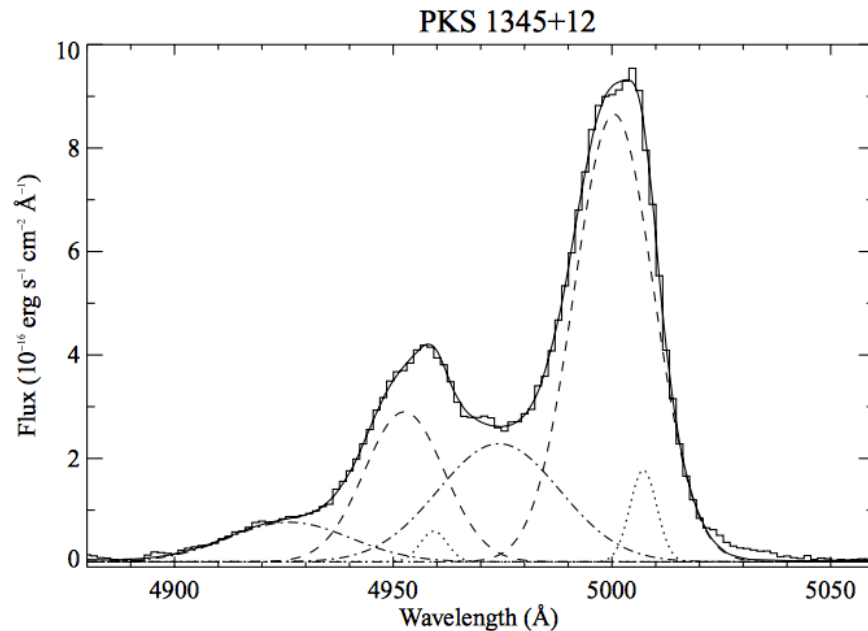
“Mechanical Feedback”

On galactic scales (<kpc), feedback not only due to disk outflows, but possibly also due to young jets! **What are the observational evidence for this?**

Compact Steep Spectrum [CSS] or Gigahertz Peaked Spectrum [GPS] objects,
Medium/Compact Symmetric Objects [MSOs/CSOs].



Jet-driven warm ionised outflows



Holt et al. (2008):

In the nuclear apertures we observe broad, highly complex emission-line profiles. Multiple Gaussian modelling of the [OIII] λ 5007 line reveals between two and four components which can have velocity widths and blueshifts relative to the halo of up to ~ 2000 km/s. We interpret these broad, blueshifted components as jet-driven outflows. Comparisons with samples in the literature show that compact radio sources harbour more extreme nuclear kinematics than their extended counterparts.

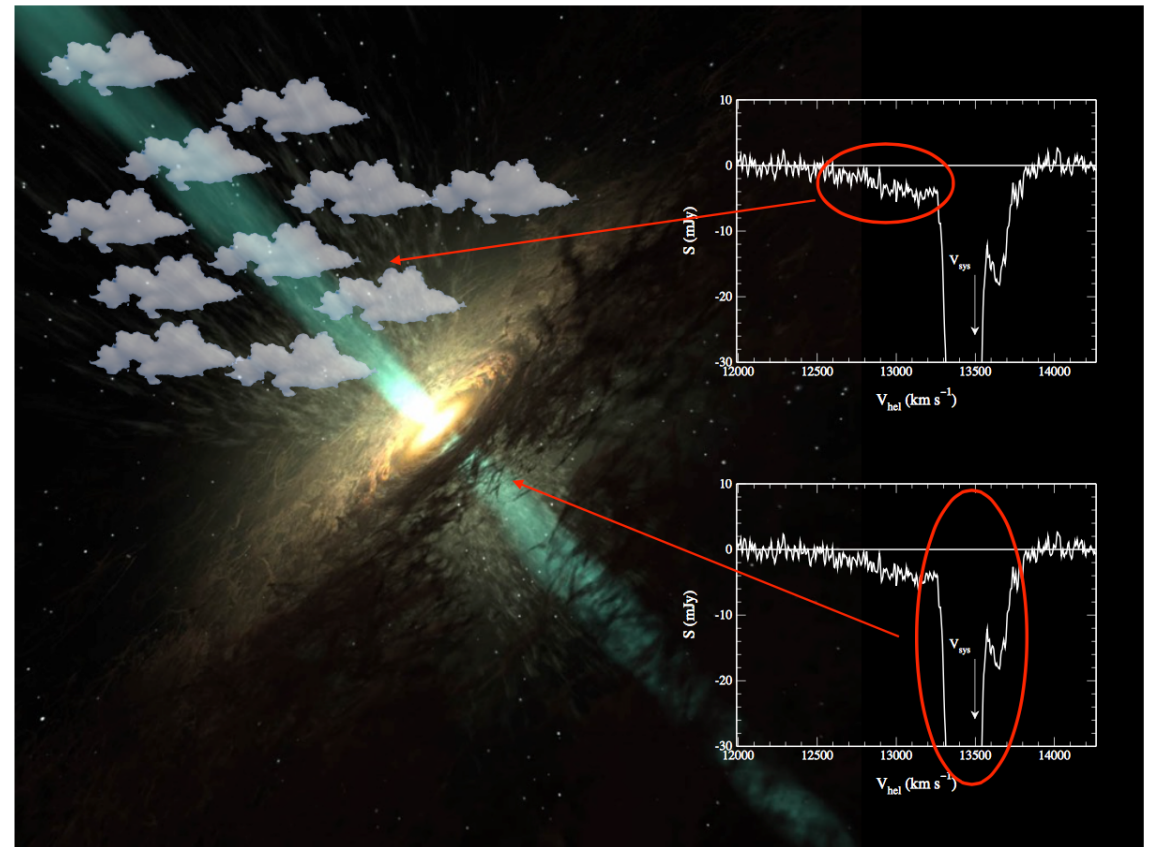
	PKS1345+12 ($z = 0.122$)	PKS1549-79 ($z = 0.152$)
$P_{5\text{ GHz}}$ (W Hz $^{-1}$)	5×10^{26}	10^{27}
\dot{M} ($M_{\odot} \text{ yr}^{-1}$)	$7.1^{+2.0}_{-2.6}$	0.12–12
$\dot{E}/10^{40}$ (erg s $^{-1}$)	350^{+150}_{-110}	5–500
(\dot{E}/L_{bol}) (%)	0.13 ± 0.01	0.0002–0.02

Jet-driven neutral atomic outflows

Morganti & Oosterloo 2018, A&A Rev

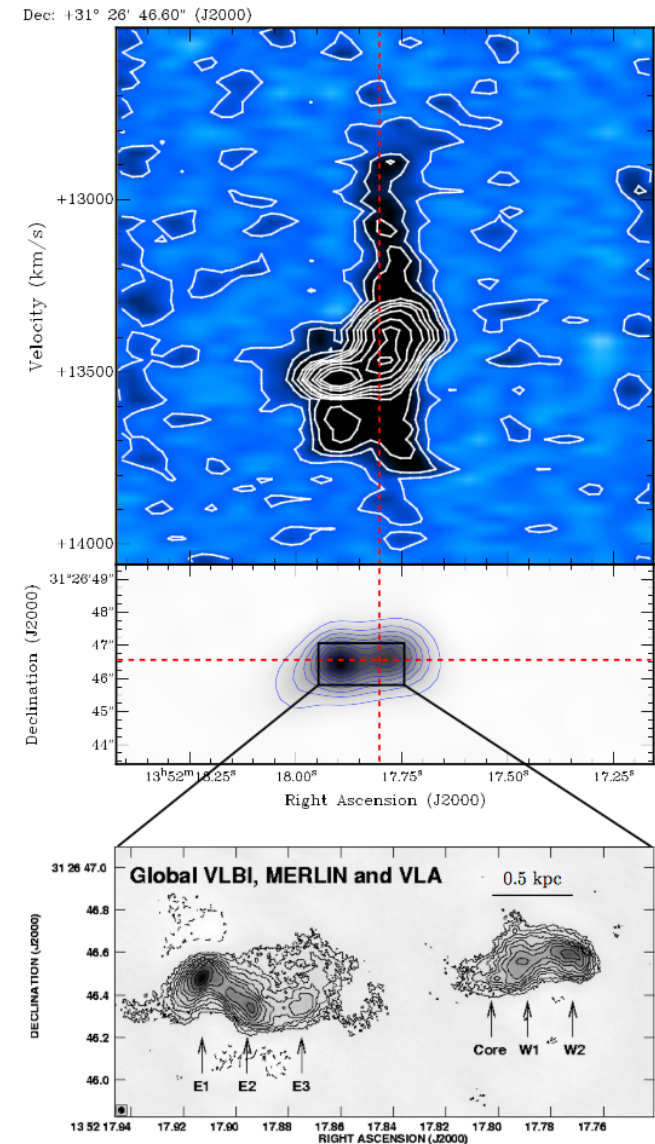
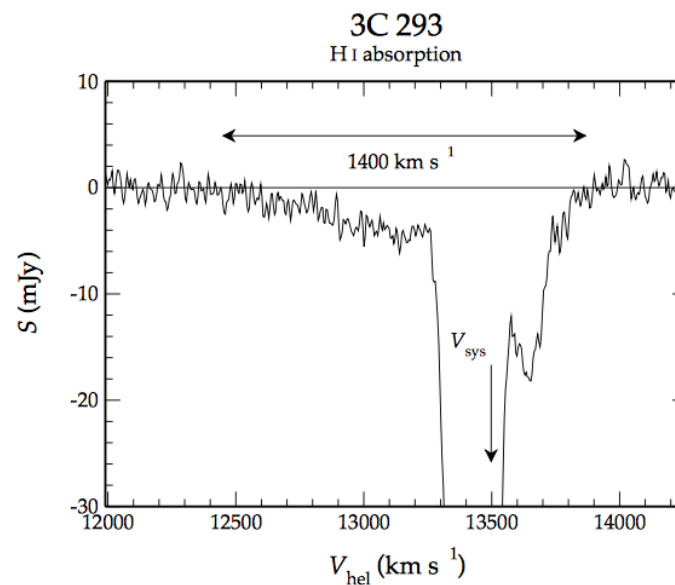
fast (> 1000 km/s) outflows of atomic hydrogen discovered via hyperfine transition of atomic hydrogen at a rest-frame frequency of 1.42GHz (or wavelength $\lambda = 21.1$ cm). Such outflows were identified through the discovery of very broad, blueshifted and typically shallow absorption wings in the spectra of active galaxies. Such velocities are much larger than typical rotational velocities and thus cannot be associated with rotating gas structures.

Source name	FWZI km s ⁻¹	\dot{M} M_{\odot} yr ⁻¹	Ref.
IC 5063	750	35	Morganti et al. (1998)
3C 190	600	-	Ishwara-Chandra et al. (2003)
3C 293	1400	8-50	Morganti et al. (2003); Mahony et al. (2013)
3C 305	800	12	Morganti et al. (2005a,b)
3C 236	1400	47	Morganti et al. (2005a)
4C 12.50	1400	8-21	Morganti et al. (2005a, 2013)
NGC 1266	400	13 ¹	Alatalo et al. (2011); Nyland et al. (2013)
OQ 208	1200	1.2	Morganti et al. (2005a)
4C 52+37	674 ²	4	Geréb et al. (2015), Schulz et al. in prep.
3C 459	600	5.5	Morganti et al. (2005a)
4C 31.06	700	-	unpublished (Morganti in prep)
1504+377	600	12	Kanekar and Chengalur (2008)
TXS 1200+045	600	32	Aditya et al. (2018)
TXS 1245 – 197	1100	18	Aditya et al. (2018)
Mrk 231	1300	8-18	Morganti et al. (2016), Teng13
NGC 3079	600	0.2-2.5	Gallimore et al. (1994); Shafi et al. (2015)
NGC 1068	300 ³	-	Gallimore et al. (1994)
4C37.11	1200	-	candidate binary BH Maness et al. (2004) Morganti et al. (2009b); Rodriguez et al. (2009)
NGC 6420	780	-	Baan et al. (1985); Beswick et al. (2001)

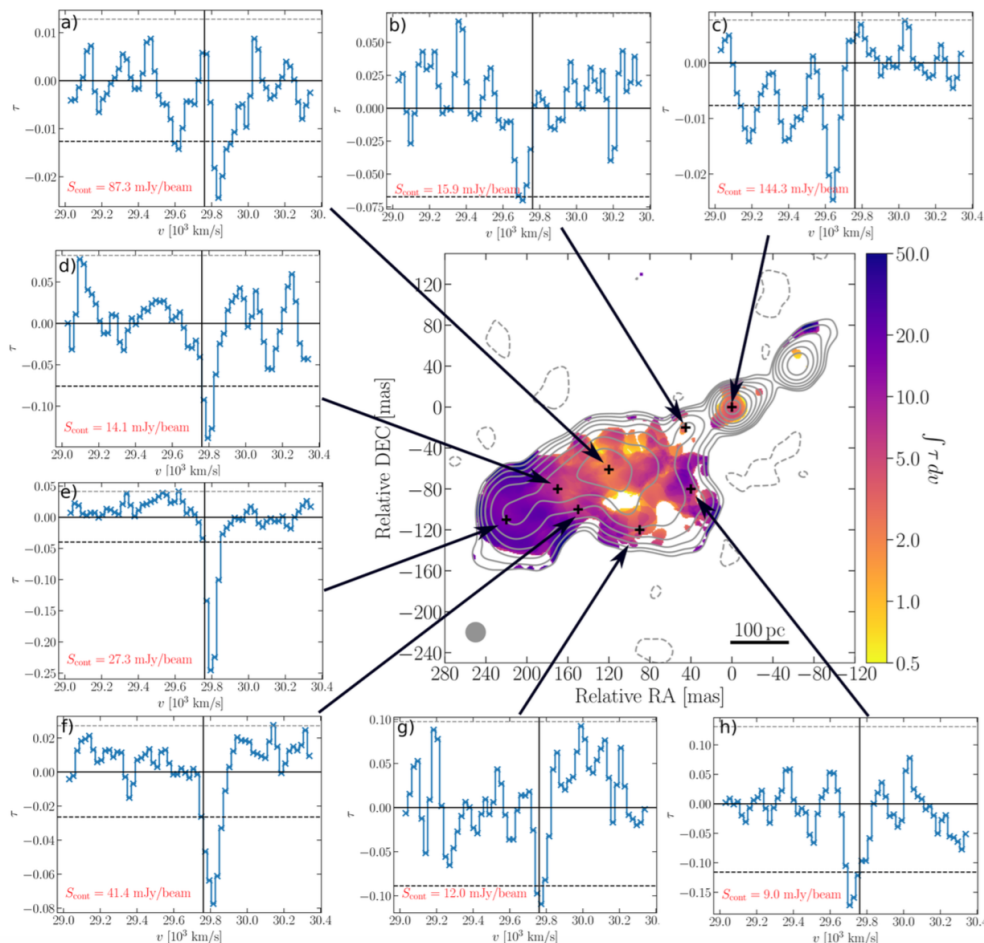


Jet-driven neutral atomic outflows

Left: Integrated H I absorption profile obtained from the WSRT (Morganti et al. 2003) showing a very broad, blueshifted wing, indicating a fast H I outflow, in addition to the deep absorption profile near the systemic velocity due to the large-scale gas disk in the object. **Right Top:** Position-velocity diagram extracted along the radio axis of the continuum source of 3C293 as obtained with the VLA, showing that the outflow is associated with the western lobe of this radio galaxy (from Mahony et al. 2013). **Middle:** The continuum image of 3C293 from these VLA observations with a resolution of 1 arcsecond. The horizontal red line marks the axis along which the position-velocity diagram was extracted while the vertical red line indicates the position of the core as determined from the VLBI image in the bottom panel. **Bottom:** the combined 1.4-GHz global VLBI, MERLIN and VLA image of the central regions of 3C293 (from Beswick et al. 2004).



Jet-driven neutral atomic outflows



Schulz et al. 2018:

Clouds with masses of $\sim 10^4 M_{\odot}$ that do not follow the regular rotation of most of the HI, and coincide with the radio jet structure. Their velocities are between 150 and 640 km/s blue-shifted with respect to the velocity of the disk-related HI.

These findings suggest that the outflow is at least partly formed by clouds. The fact that 3C236 is a low excitation radio galaxy, makes it less likely that the optical AGN is able to produce strong radiative winds leaving the radio jet as the main driver for the HI outflow.

Central panel: Continuum image of the central region of 3C236.

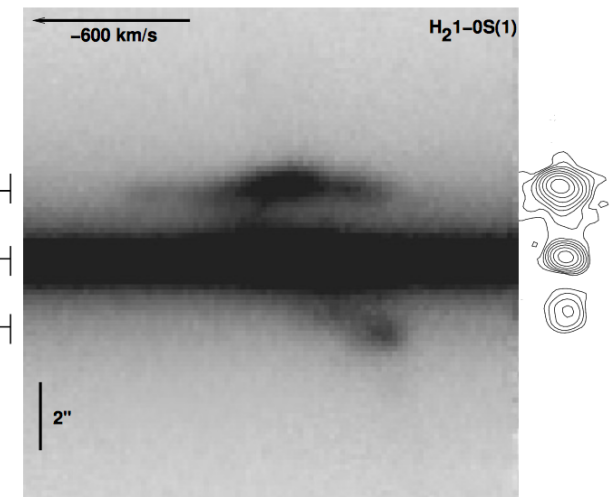
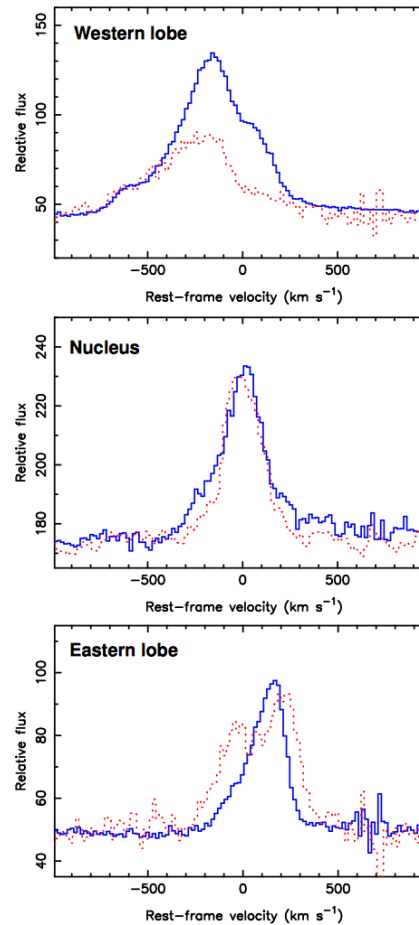
Outer panels: The optical depth spectrum shown as the ratio of the absorbed flux density to the continuum flux density. The dashed line represents the optical depth detection limit at the 3σ level. The solid, vertical line marks the systemic velocity.

Jet-driven molecular outflows

Tadhunter et al. 2014:

Near-IR spectroscopic evidence for a jet-driven molecular outflow in the nearby, radio-loud Seyfert galaxy IC 5063 ($z = 0.011$). The long-slit spectrum (right), shows clear evidence for disturbed kinematics and jet-accelerated outflows at the site of the western radio lobe; the lines are significantly narrower at other locations in the galaxy. The velocity profiles derived from spectra extracted from three spatial locations across the galaxy are presented to the left, where the solid blue lines represent the H₂1-0S(1) λ 2.128 feature, and the dotted red lines represent the Br γ feature.

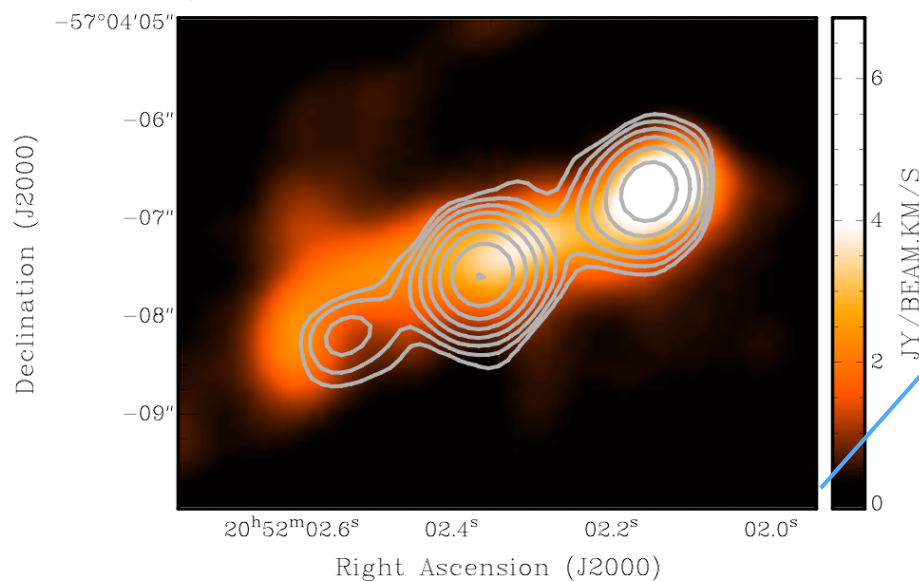
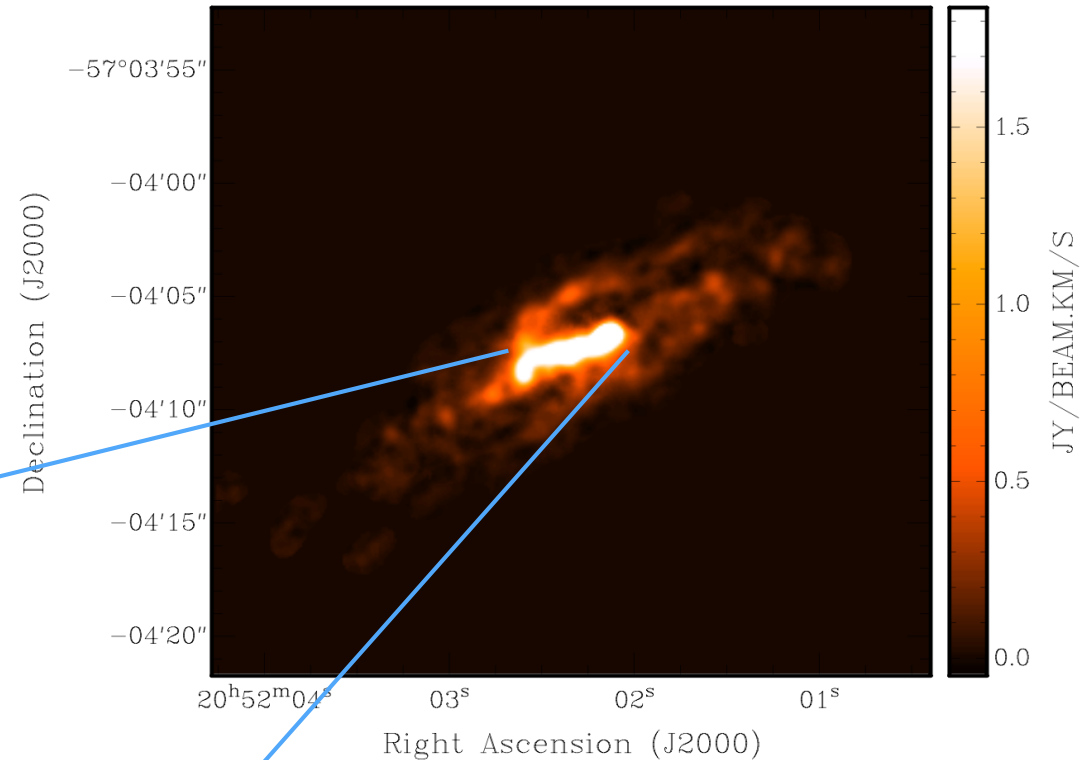
For comparison, a scaled version of the 1.4GHz radio map of the source is presented to the right.



Jet-driven molecular outflows

Morganti et al. 2015:

Total intensity image representing the distribution of the CO(2-1) in IC 5063 and showing the striking brightness contrast between the inner, bright CO and the fainter outer disk.

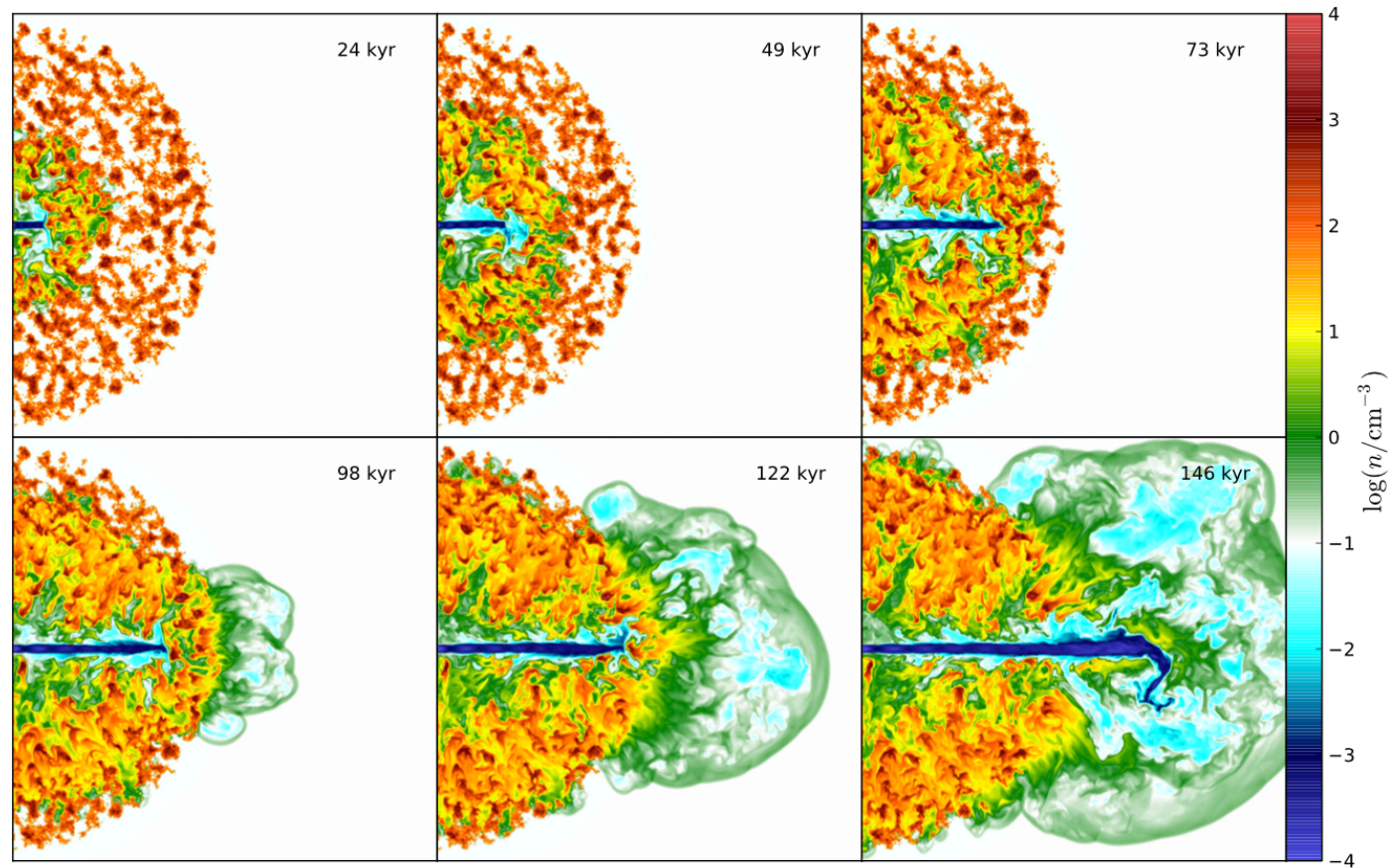


Contours of the 230 GHz continuum emission super-posed onto the central region of the total intensity of the CO(2-1) illustrating the spatial correlation between the two.

Jet-driven molecular outflows

- The observed distribution and kinematics of the cold molecular gas suggests that the a newly formed radio jet is driving the bulk of the gas outflow ($\sim 30 M_{\odot}/\text{yr}$).
- Neutral and molecular outflows are accelerated by fast shocks driven into the dense, circum-nuclear ISM by the relativistic radio jets. Rather than avoid molecular dissociation and then ionisation, the gas becomes highly ionized, compressed, accelerated and heated to temperatures of over 10^6K as it enters the shocks. The molecules in the outflow then form as the compressed, post-shock gas cools. In this scenario, the warmer molecular gas in the outflow ($\sim 2000\text{K}$), as detected in the broad wings of near-IR H_2 lines of IC 5063 (Tadhunter et al. 2014), represents the cooling phase, while the CO lines (Morganti et al. 2015) sample the reservoir of gas in the outflow that has already cooled.
- The above scenario is consistent with what is seen regarding the jet-driven feedback in young, gas-rich radio-galaxies, in a series of three-dimensional relativistic hydrodynamic simulations by Wagner et al. (2011-18), where the ISM was initialised as a two-phase fractal gas distribution consisting of a warm, dense phase of clouds with a given filling factor and maximum size, embedded in a hot, diffuse galactic halo.

Jet-ISM interactions: simulations



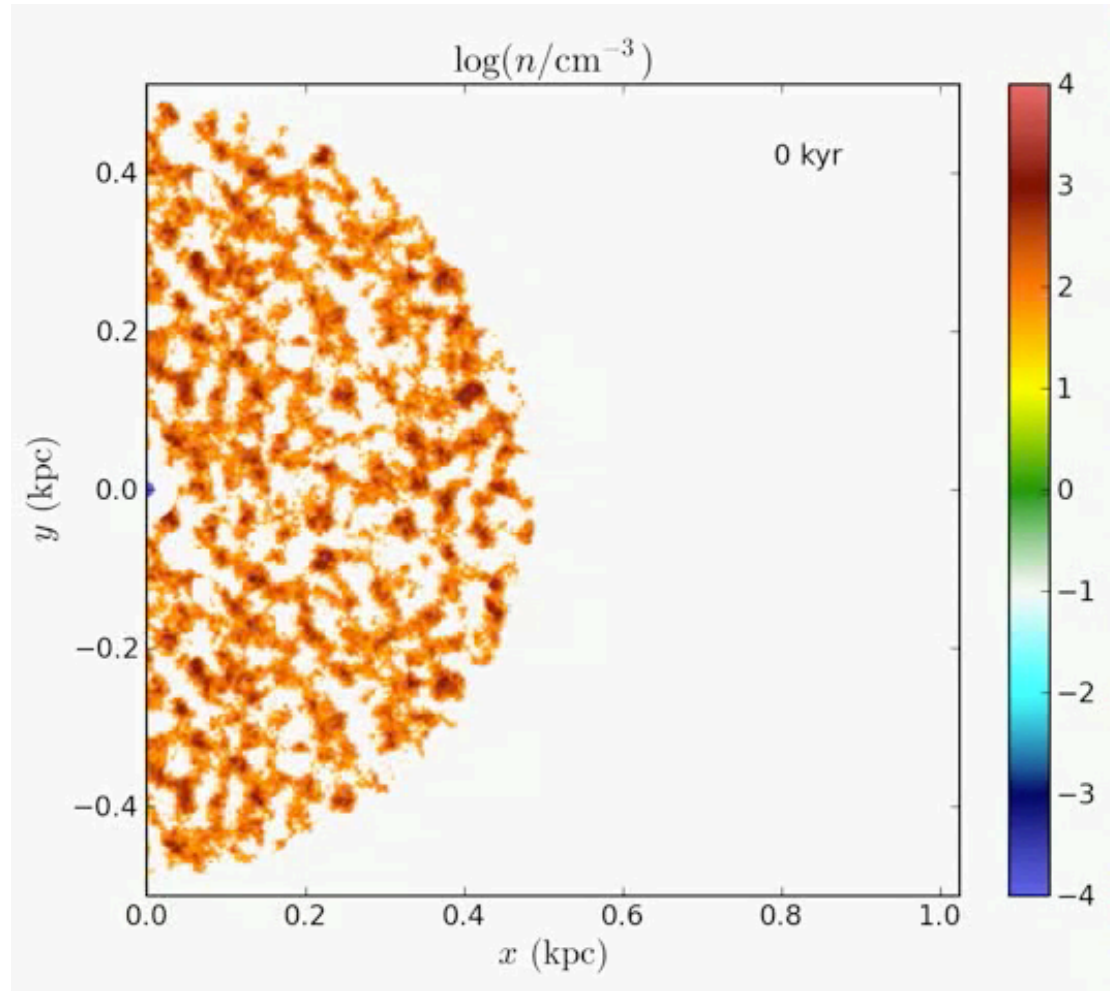
Wagner & Bicknell 2011:

The jet, while percolating through the channels of the porous clouds, dispersed clouds substantially at all radii over 4π sr solid angle, indicating that AGN jet feedback does have an effect on the dense phase in the ISM, e.g., atomic and molecular clouds. As the jet struggled through the dense field of clouds, it was deflected, split, and confined. In the process, the jet blew an energy-driven bubble through the ISM. The forward shock swept up the hot ISM and the surface of the clouds, disrupting them slightly. The primary mode of energy transfer occurred through the channel flows, which were mass-loaded through the hot ISM and gradually through surface ablation of the clouds, and carried substantial ram pressure (comparable to or a factor of a few greater than the thermal pressure). The hydrodynamic ablation of clouds was driven by the shear with the surrounding flow, which generates Kelvin-Helmholtz instabilities at the cloud interfaces. Clouds were also accelerated in bulk through direct impact of the channel flows.

$\log P_{\text{jet}}^{(a)}$	$n_h^{(b)}$	$p_{\text{ISM}}/k^{(c)}$	$\langle n_w \rangle^{(d)}$	$f_V^{(e)}$	$M_{w,\text{tot}}^{(f)}$
(erg)	(cm^{-3})	($\text{cm}^{-3} \text{K}$)	(cm^{-3})		($10^9 M_\odot$)
45	0.1	10^6	100	0.42	1.6

(a)Jet power. (b)Density of the hot phase. (c) p/k of both hot and warm phases. (d)Average density of the warm phase.

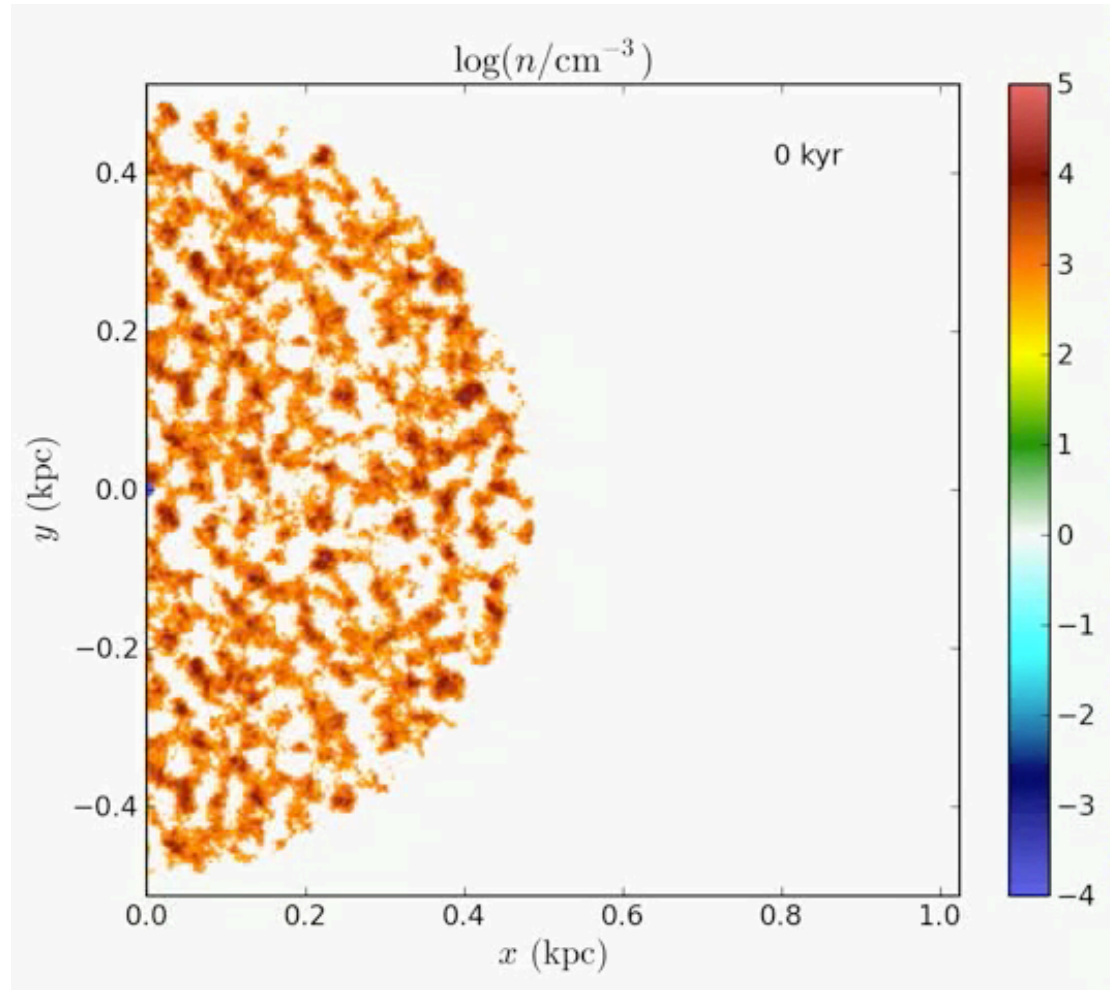
(e)Volume filling factor of the warm phase. (f)Total mass in the warm phase.



$\log P_{\text{jet}}^{(a)}$	$n_h^{(b)}$	$p_{\text{ISM}}/k^{(c)}$	$\langle n_w \rangle^{(d)}$	$f_V^{(e)}$	$M_{w,\text{tot}}^{(f)}$
(erg)	(cm^{-3})	($\text{cm}^{-3} \text{K}$)	(cm^{-3})		($10^9 M_\odot$)
44	1.0	10^7	1000	0.42	16

(a)Jet power. (b)Density of the hot phase. (c) p/k of both hot and warm phases. (d)Average density of the warm phase.

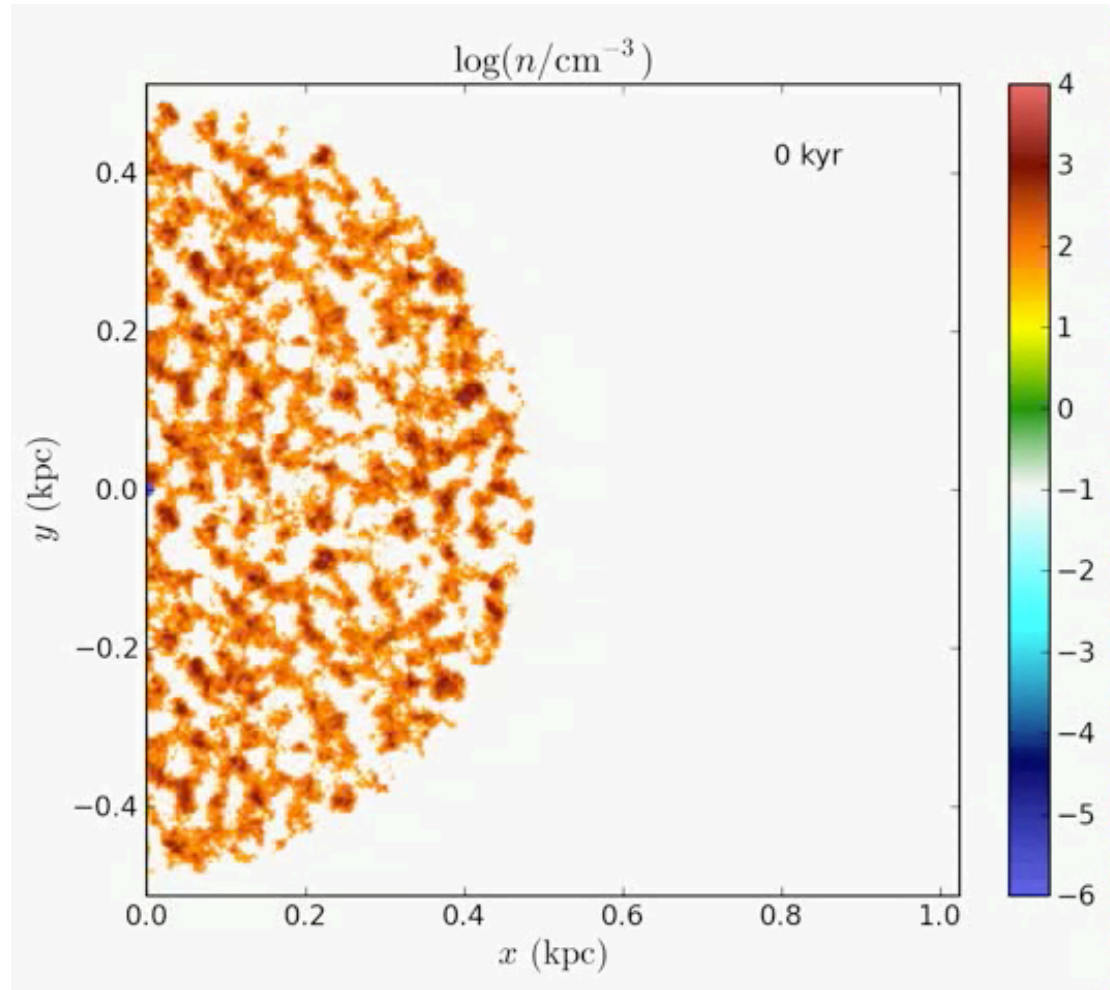
(e)Volume filling factor of the warm phase. (f)Total mass in the warm phase.



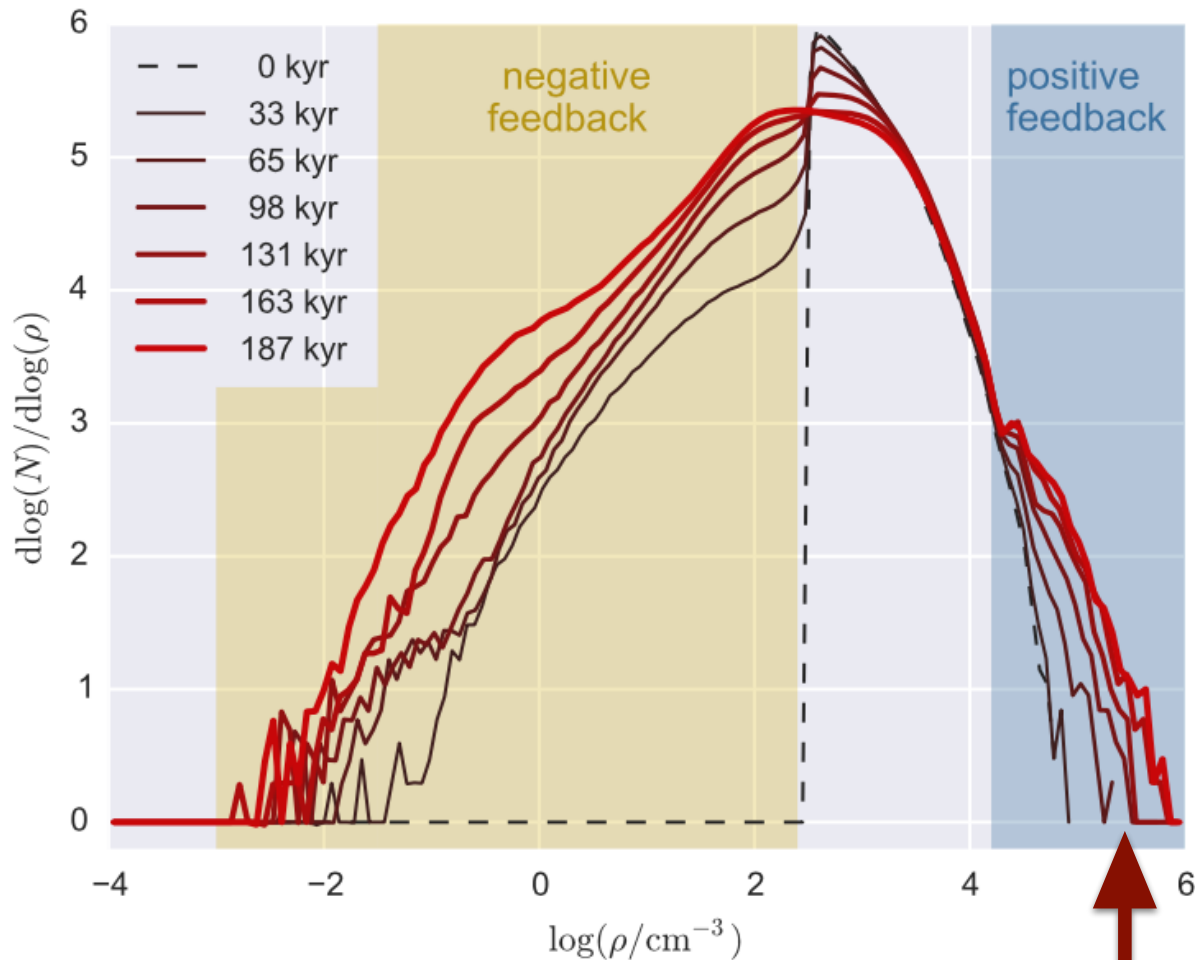
$\log P_{\text{jet}}^{(a)}$	$n_h^{(b)}$	$p_{\text{ISM}}/k^{(c)}$	$\langle n_w \rangle^{(d)}$	$f_V^{(e)}$	$M_{w,\text{tot}}^{(f)}$
(erg)	(cm^{-3})	($\text{cm}^{-3} \text{K}$)	(cm^{-3})		($10^9 M_\odot$)

43 0.1 10^6 100 0.42 1.6

(a)Jet power. (b)Density of the hot phase. (c) p/k of both hot and warm phases. (d)Average density of the warm phase.
(e)Volume filling factor of the warm phase. (f)Total mass in the warm phase.



Positive vs negative feedback



Wagner et al. 2012:

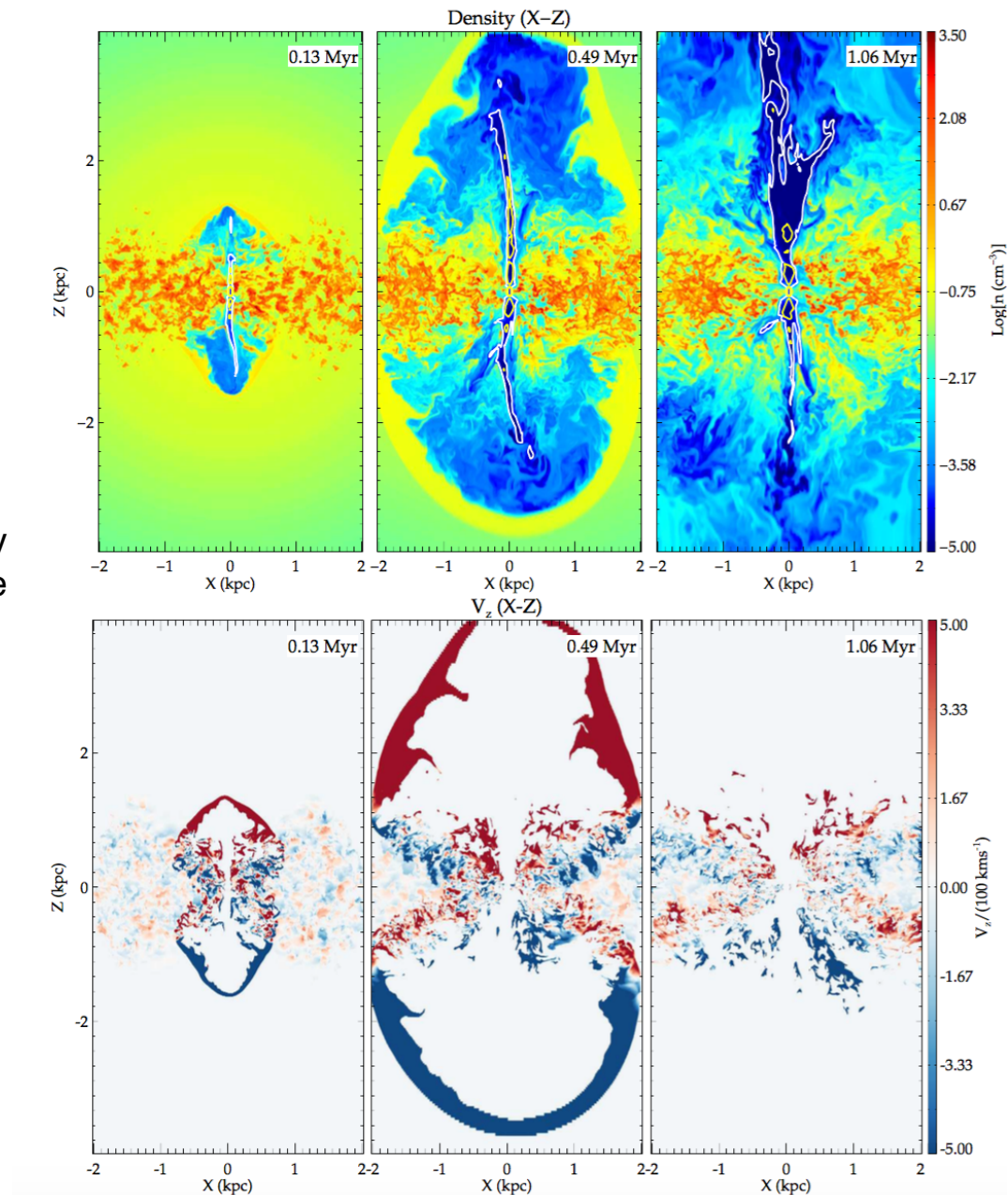
The most important parameter determining the efficiency of negative feedback was the maximum size of clouds, or, equivalently, their maximum column density. For a fixed volume filling factor, and total mass, the smaller the clouds, the easier they were to disperse because the ratio of surface area subjected to the KH instability and ablation increases in relation to the mass of the cloud. Conversely, bigger clouds were harder to disperse, but were, instead, more susceptible to collapse and induced star formation.

shock compression

Positive vs negative feedback

Mukherjee et al. 2018 :

Shocks driven directly by the jet and the jet-driven energy bubble raise the velocity dispersion throughout the disk by several times its initial value. Compression by the jet-driven shocks can enhance the star formation rate in the disk, especially in a ring-like geometry close to the axis. However, enhanced turbulent dispersion in the disk also leads to quenching of star formation. Whether positive or negative feedback dominates depends on jet power, ISM density, jet orientation with respect to the disc, and the time-scale under consideration.



Clusters of Galaxies

- cooling flows

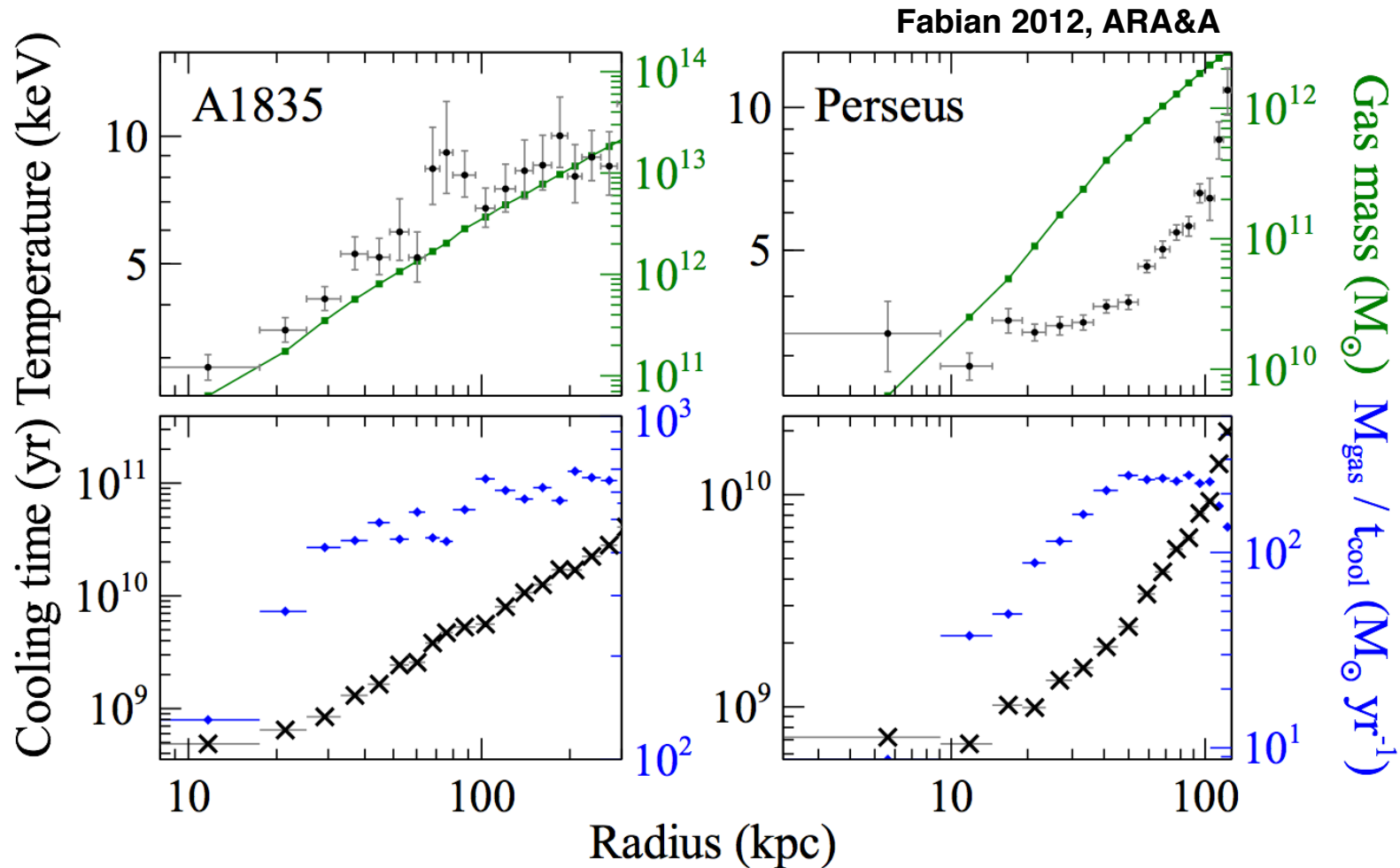
Fabian 1994:

A cooling flow cluster is characterized by bright X-ray emission from cool, dense gas in the central region of the cluster. Within the cooling radius, the surface brightness of the gas near a central cD galaxy often rises dramatically by factors of up to 100, corresponding to a rise in gas density by factors of 10 or more. The X-ray luminosity within the cooling region reaches values of 10^{45} erg/s in the extreme. In many cases it is more than 10% of the cluster's total luminosity.

If this luminosity is uncompensated by heating, the gas will radiate away its thermal and gravitational energy on a timescale of <1 Gyr. As the gas radiates, its entropy decreases and it is compressed by the surrounding gas, causing it to flow inward. The cooling time decreases as the gas density increases and, eventually, the gas temperature drops rapidly to $< 10^4$ K, so that cooled gas condenses onto the central galaxy. The condensing gas is replenished by hot gas lying above, leading to a steady, long-lived, pressure-driven inward flow of gas at a rate of up to $1,000 M_{\odot}/\text{yr}$.

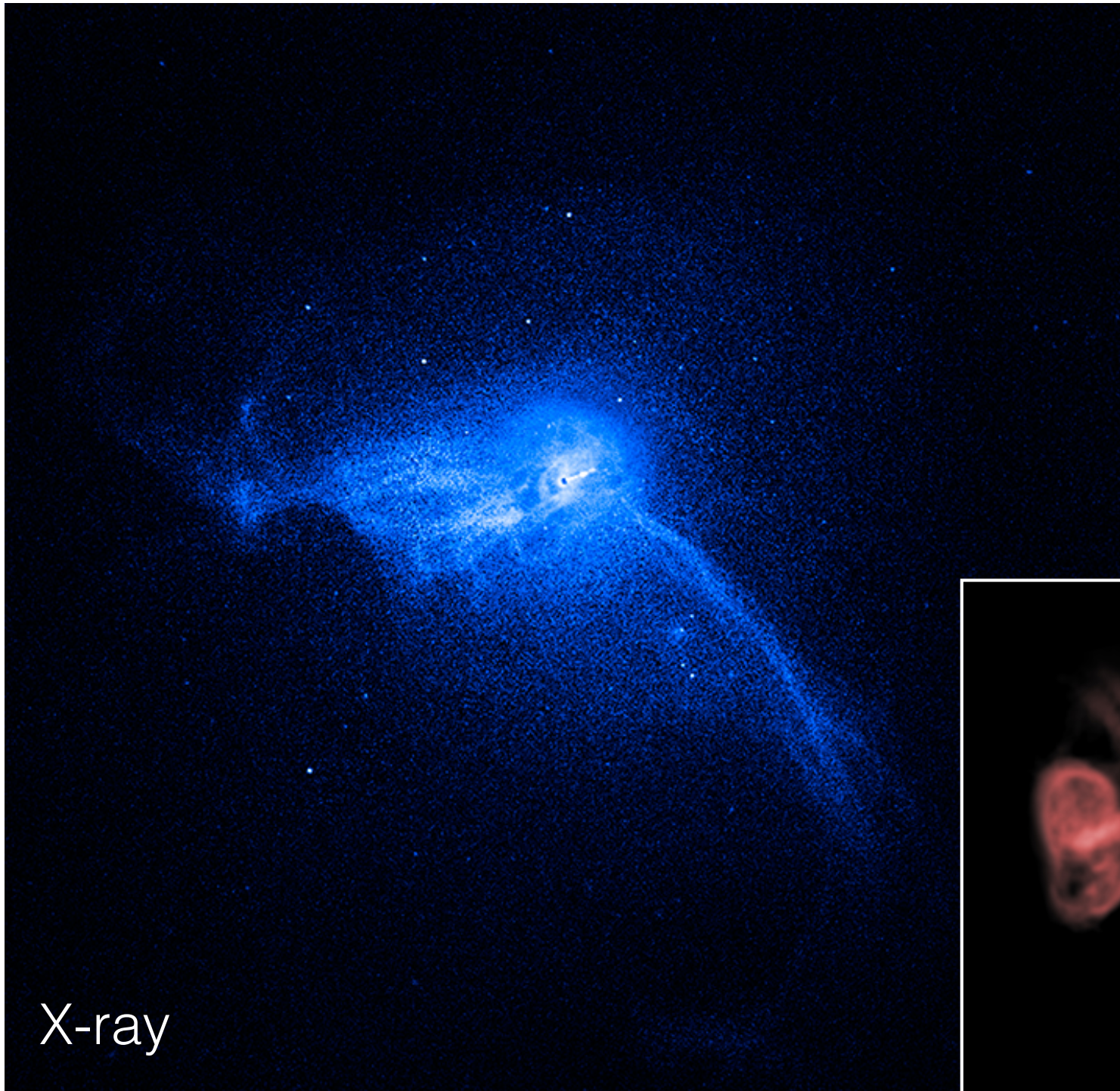
$$t_{\text{cool}} \equiv \frac{\frac{5}{2}nkT}{n^2\Lambda}$$

AGN (jet) heating?

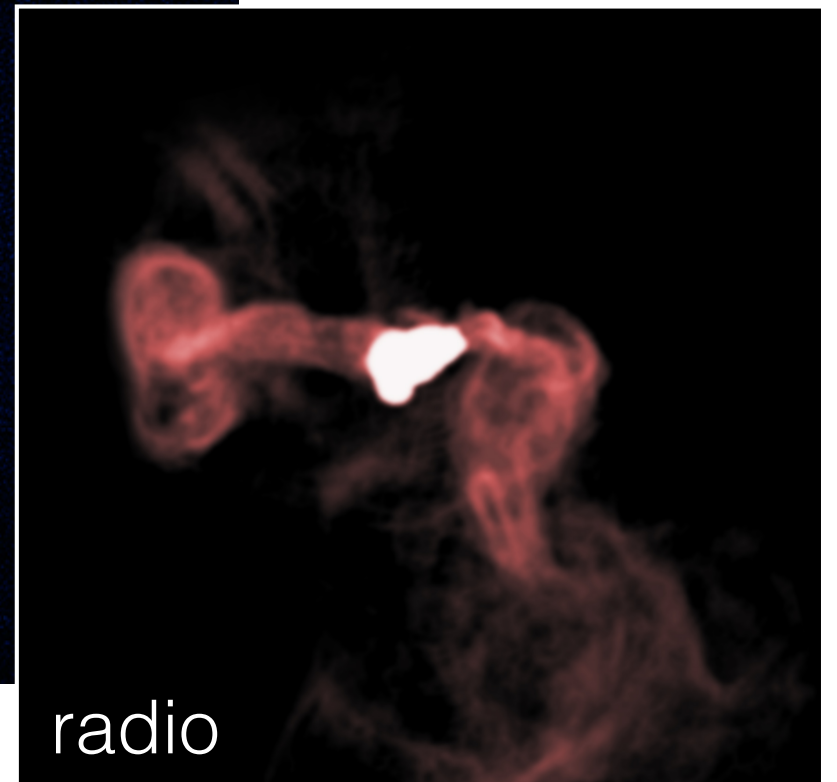


The failure to find large quantities of cooling gas with the expected properties of a cooling flow implies that more than 90% of the energy radiated away is being replenished. Only a few percent of the gas associated with the cooling flow forms stars and even less accretes onto the central supermassive black hole. For an AGN to be a viable agent, it must be powerful, persistent, an efficient heater, and it must distribute the heat throughout the cooling region.

Virgo / M87

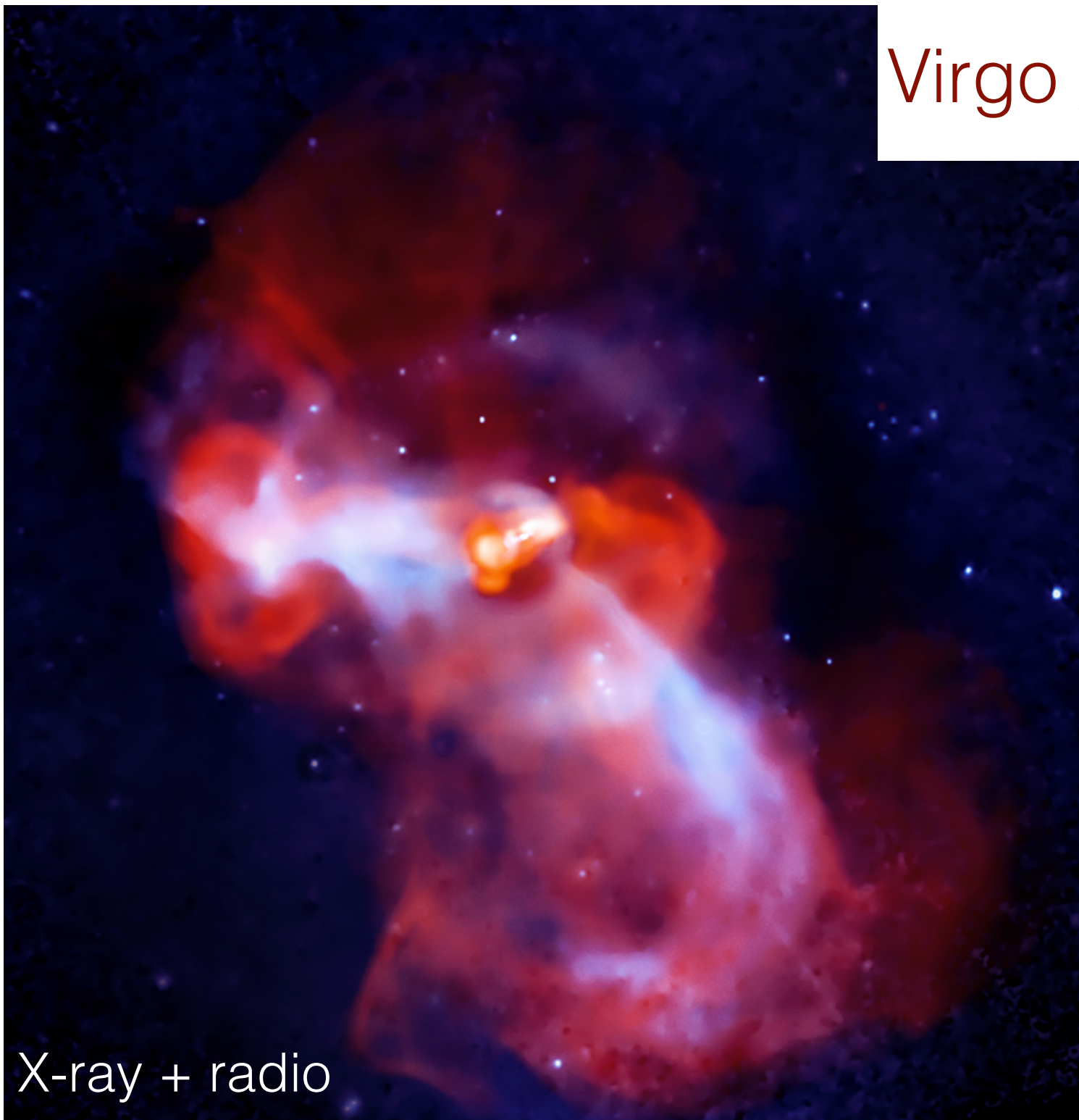


X-ray



radio

Virgo / M87



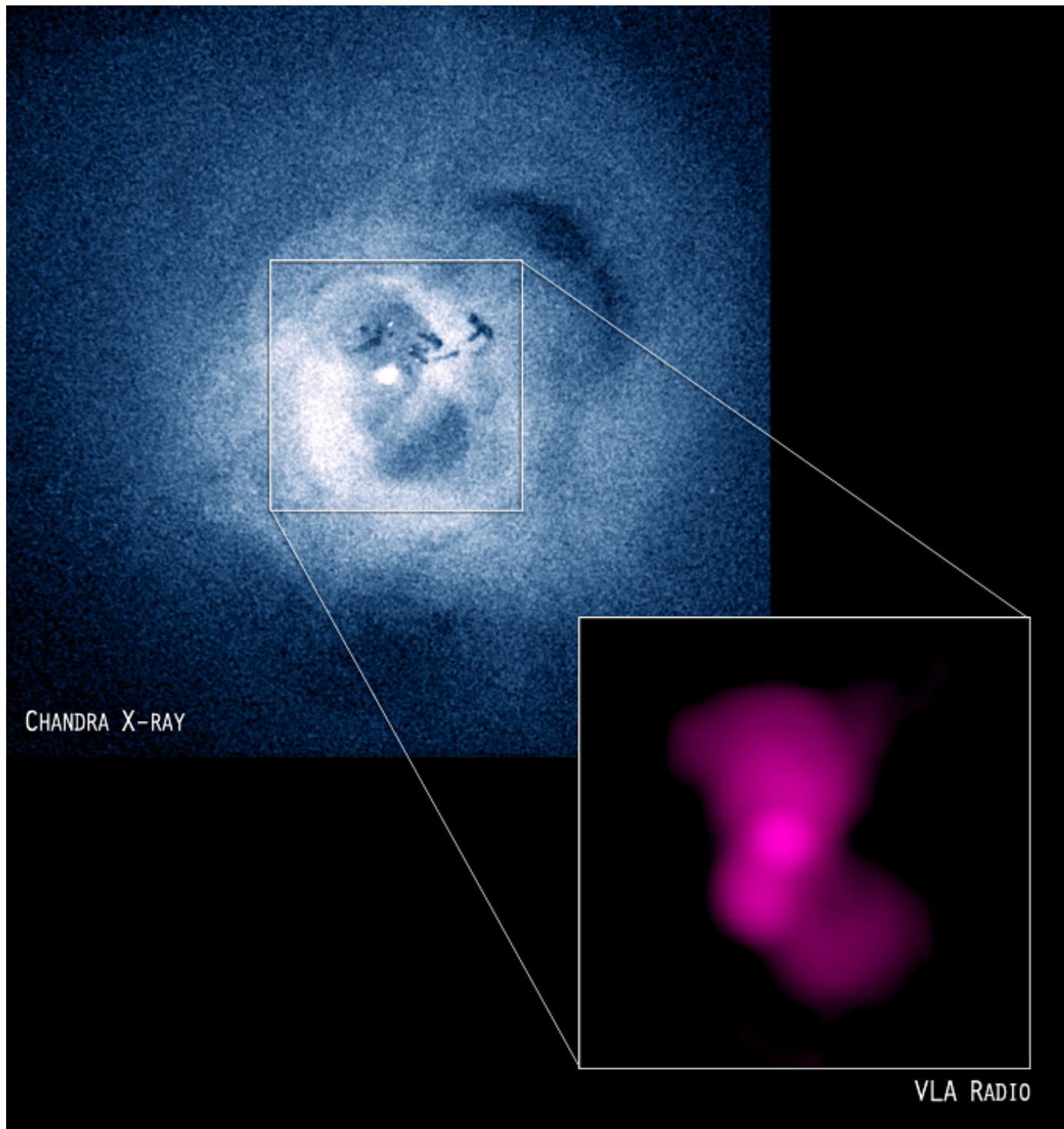
X-ray + radio

Perseus/
3C 84

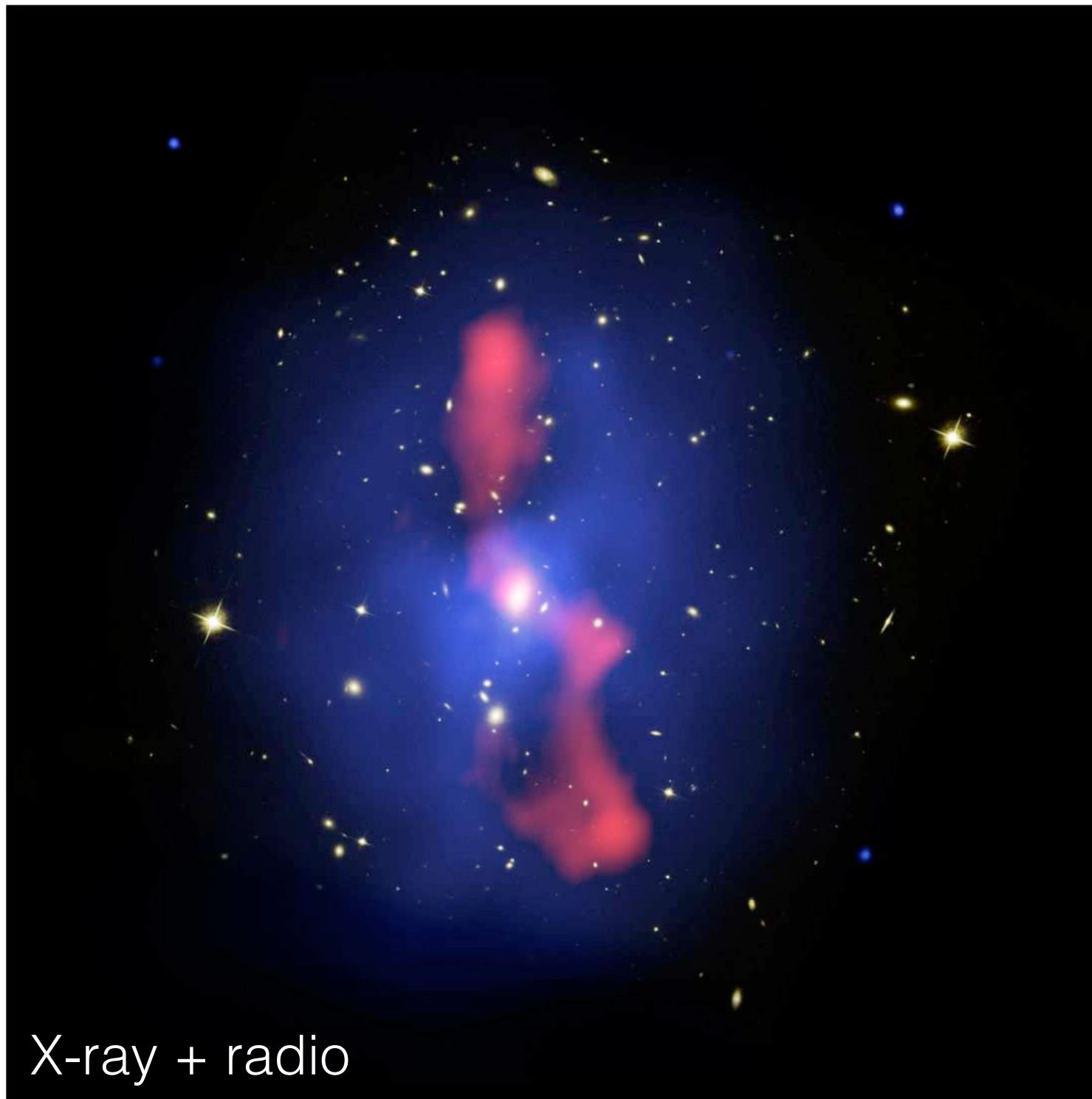
X-ray

This is an X-ray image of the Perseus galaxy cluster, also known as 3C 84. The image shows a bright, multi-layered central core with a complex, filamentary structure. The core is surrounded by a diffuse, multi-phase emission that extends outwards, appearing as a series of concentric, irregular shells. The color gradient ranges from dark red at the periphery to bright yellow and white at the center, indicating a temperature gradient. The overall appearance is that of a rich, multi-phase intracluster medium.

Perseus/ 3C 84

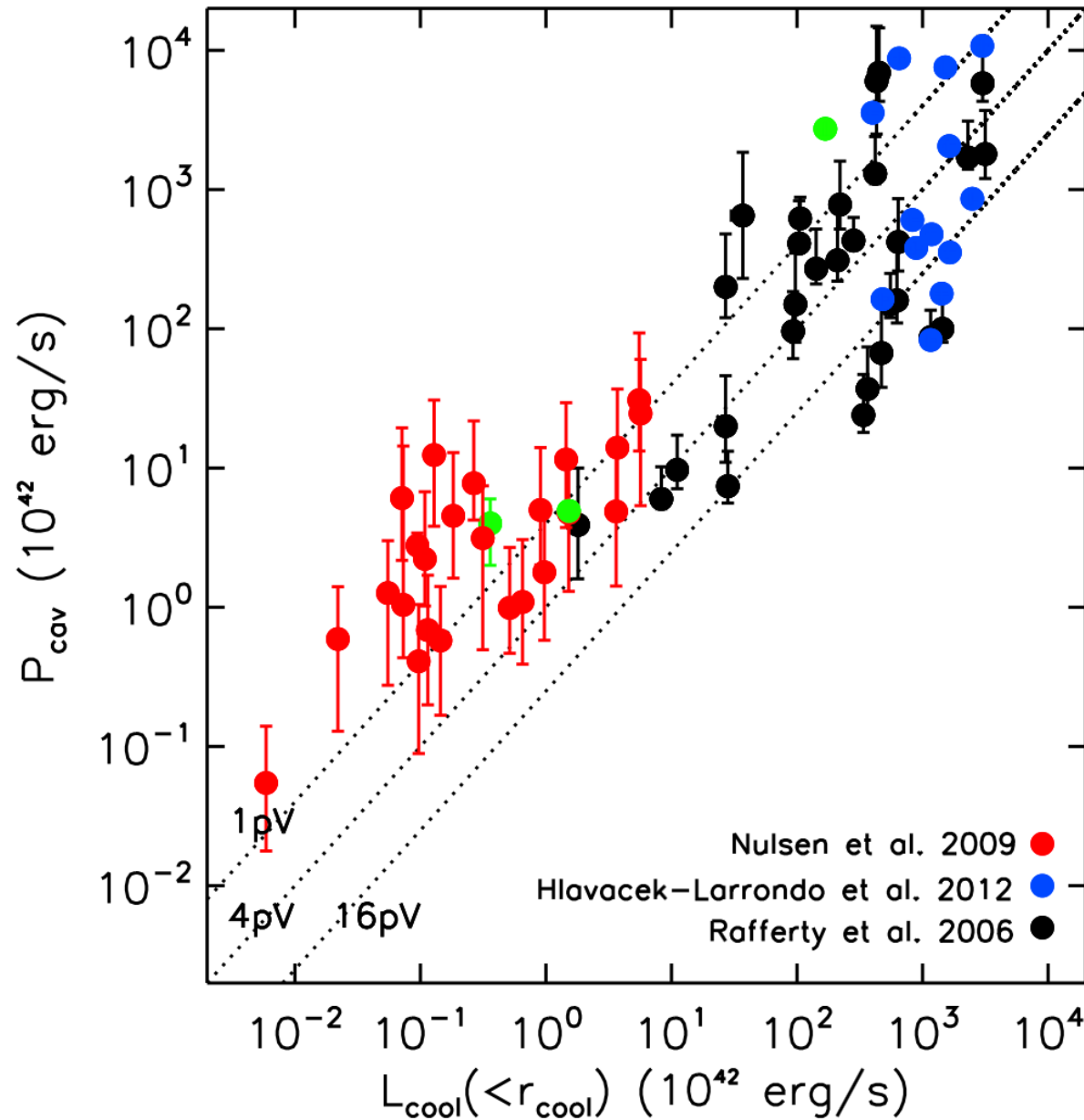


MS0735.6
+7421



X-ray + radio

Cluster cavities



Fabian 2012, ARA&A

Power inferred from cavities/bubbles plotted against luminosity within the cooling region (where the radiative cooling time is less than 7 Gyr). The objects range from luminous clusters, through groups, to elliptical galaxies.

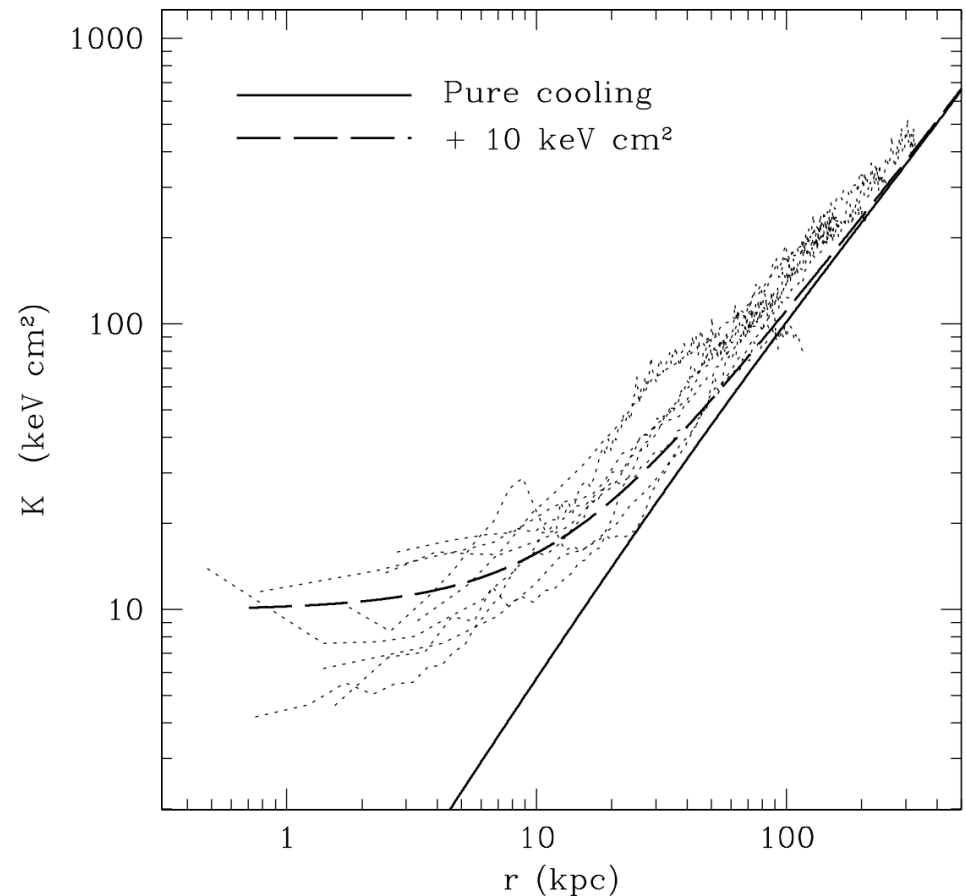
AGN (jet) heating

McNamara & Nulsen 2007, ARA&A

A true AGN feedback loop, as opposed to simple AGN heating, must couple the AGN energy output to the reservoir of gas fuelling it. In other words, the X-ray luminosity of the cooling gas measured on tens of kiloparsec scales, and the jet power maintained by accretion of gas near the AGN on subparsec scales, are apparently in causal contact.

The most powerful AGN in clusters do not dramatically raise the temperature or lower the density of the gas in their vicinity. Instead, they raise the central entropy of the gas through a surprisingly gentle “heating” process that restores potential energy to the atmosphere that was lost by radiation. This entropy boost is shown as a flattening of the central atmospheric entropy profiles compared to a pure cooling atmosphere (Voit & Donahue 2005) and in the correlation between jet power and the value of the central entropy of the host’s hot atmosphere.

Voit & Donahue 2005



How exactly does it work?

- Expected strong shocks driven in the surrounding medium by the expanding jet cocoons (Clarke +97, Heinz +98, Kaiser & Alexander 99)
- ...but no signatures of such have been found in the first high-resolution Chandra exposures... **This led to the idea of**
- Transonic expansion of short-lived lobes, rising in the cluster atmosphere in a form of buoyant bubbles, converting **somehow** their enthalpy to the gas kinetic energy (e.g., Churazov +01, Fabian +03, Ruszkowski +04)

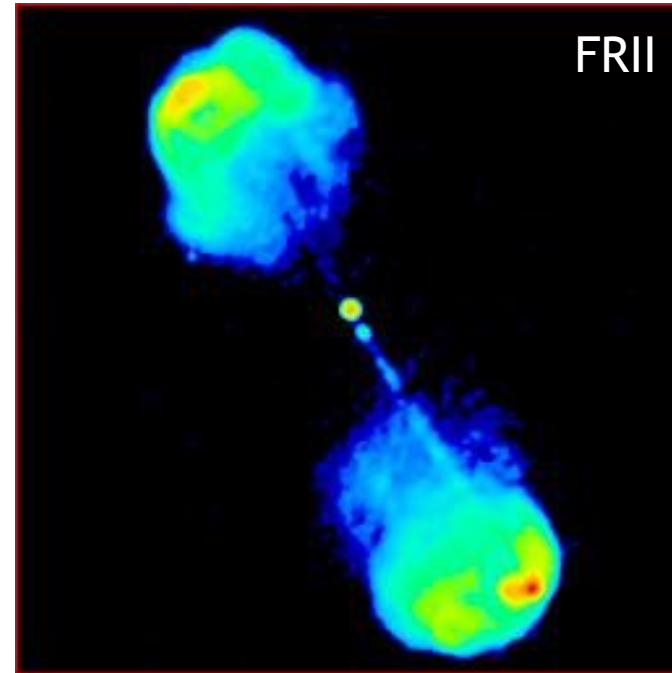
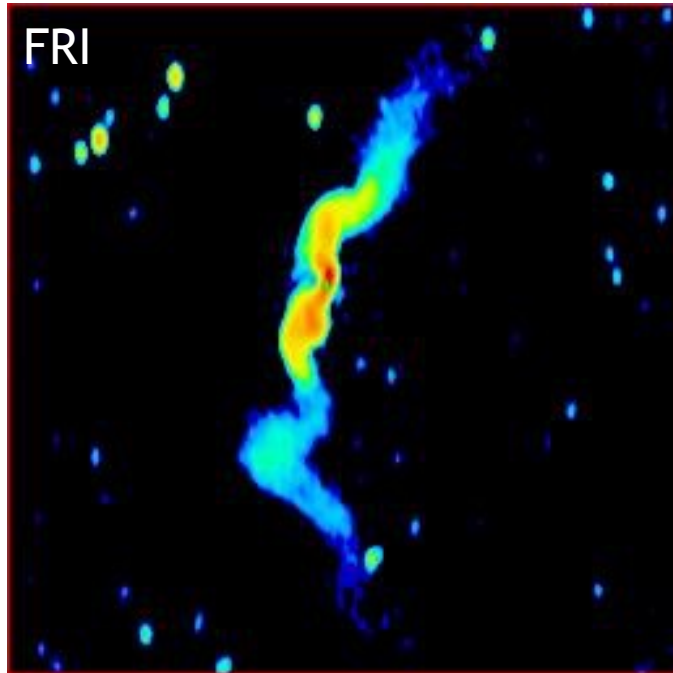
How exactly does it work?

- Expected strong shocks driven in the surrounding medium by the expanding jet cocoons (Clarke +97, Heinz +98, Kaiser & Alexander 99)
- ...but no signatures of such have been found in the first high-resolution Chandra exposures... **This led to the idea of**
- Transonic expansion of short-lived lobes, rising in the cluster atmosphere in a form of buoyant bubbles, converting **somehow** their enthalpy to the gas kinetic energy (e.g., Churazov +01, Fabian +03, Ruszkowski +04)

However...

- Details of the related energy dissipation processes quite controversial
- Stability of buoyant bubbles in the ICM quite problematic (e.g., Jones & DeYoung 05, Diehl +08, O'Neil +09)
- Weak shocks associated with large-scale lobes in galaxy clusters finally found in deep Chandra and XMM-Newton exposures of various systems (McNamara +05, Gitti +07, 11, Nulsen +05a, 05b, Fabian +06, Wise +07, Simionescu +07, 09, Forman +05, 07, Wilson +06, Reynolds +08, Cavagnolo +11, Blanton +11, Lal +10; also Kraft +07, Croston +07, 09, Jetha +08, Gitti +10, Randall +11, Siemiginowska +12, Shelton +11)

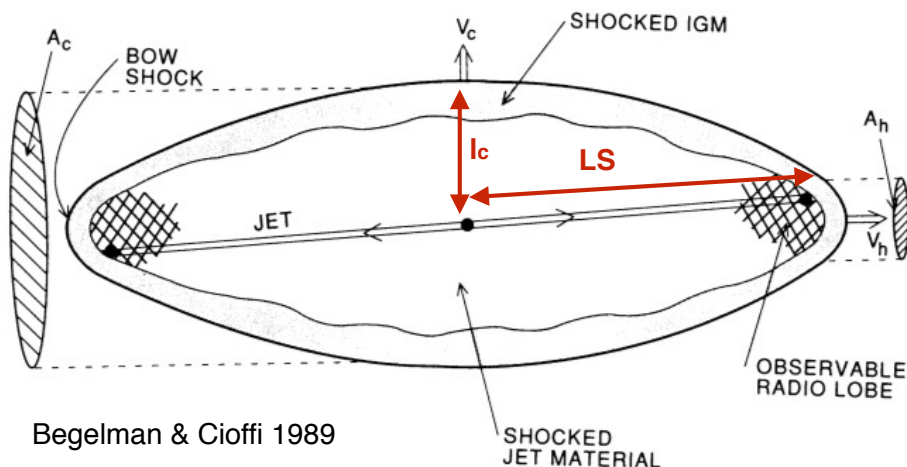
FRI versus FR II radio sources



- FRII radio sources are on average more luminous in radio than FRIs; large-scale morphologies of their radio lobes are consistent with a supersonic expansion, in contrast to the (trans)-sonic expansion of FRI-type plume structures
- At lower redshifts FRIIs seem to avoid dense cluster environment (Wan & Daly 96; Zirbel 97; Harvanek & Stocke 02; Slee +08; Wing & Blanton 11)
- At higher redshifts, however, FRIIs are found also in rich systems (Yates +89; Hill & Lilly 91; Siemiginowska +05; Belsole +07; Antognini +12)

Why should we care about FRIsIs?

- Long-term evolution of FRIs (“classical doubles”) is very well understood, and tested in many different numerical simulations (Begelman & Cioffi 89, Kaiser & Alexander 97, Komissarov & Falle 98), unlike the long-term evolution of FRIs...
- Local luminous FRIs may be more representative for the high-z universe than weak FRIs
- Efficient heating of the ICM, suppression of the starformation in the evolving galaxies, or regulating the SMBH growth, requires powerful jets of the FRII type, with $L_j \geq 1e45$ erg/s and $t_j \geq 10$ Myr (Voit & Donahue 05, Matthews & Guo 11, Antognini +12)



$$L_j = c \rho(LS) v_h^2 A_h \quad , \quad p = \rho(l_c) v_c^2 \quad , \quad 3pV = 2L_j t \quad ,$$

$$v_h = \frac{dLS}{dt} \quad , \quad v_c = \frac{dl_c}{dt} \quad , \quad \frac{dV}{dt} = 2\pi l_c^2 v_h \quad .$$

Why should we care about FR IIs?

- Long-term evolution of FR IIs (“classical doubles”) is very well understood, and tested in many different numerical simulations (Begelman & Cioffi 89, Kaiser & Alexander 97, Komissarov & Falle 98), unlike the long-term evolution of FR I...
- Local luminous FR IIs may be more representative for the high-z universe than weak FR I
- Efficient heating of the ICM, suppression of the starformation in the evolving galaxies, or regulating the SMBH growth, requires powerful jets of the FR II type, with $L_j \geq 1e45 \text{ erg/s}$ and $t_j \geq 10 \text{ Myr}$ (Voit & Donahue 05, Matthews & Guo 11, Antognini +12)

One should keep in mind that

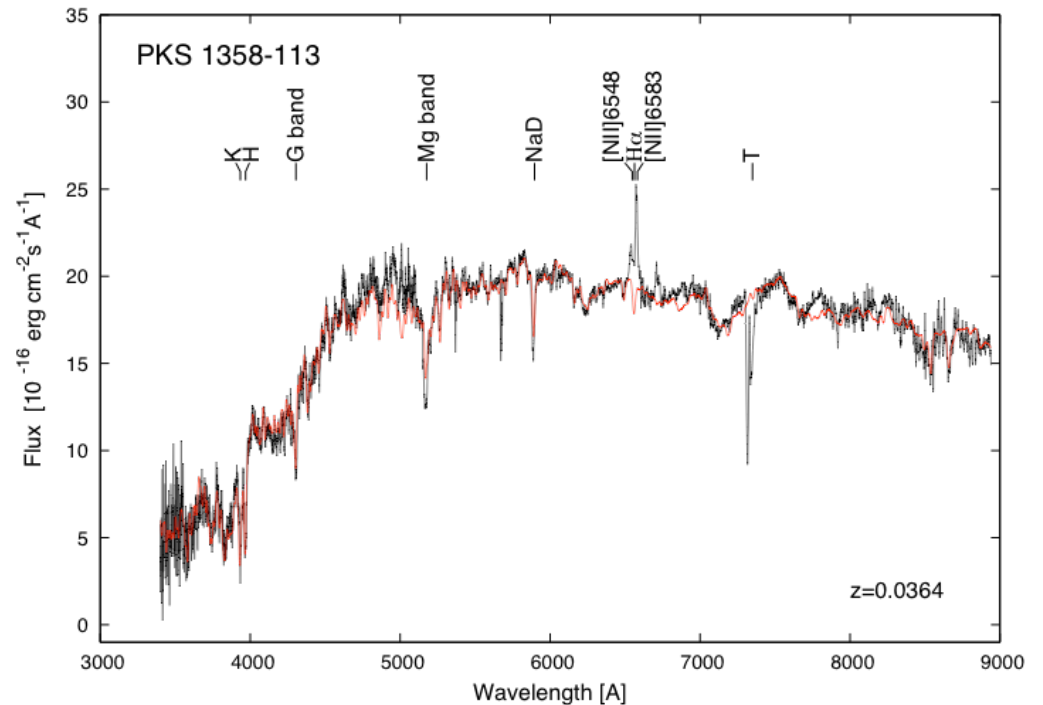
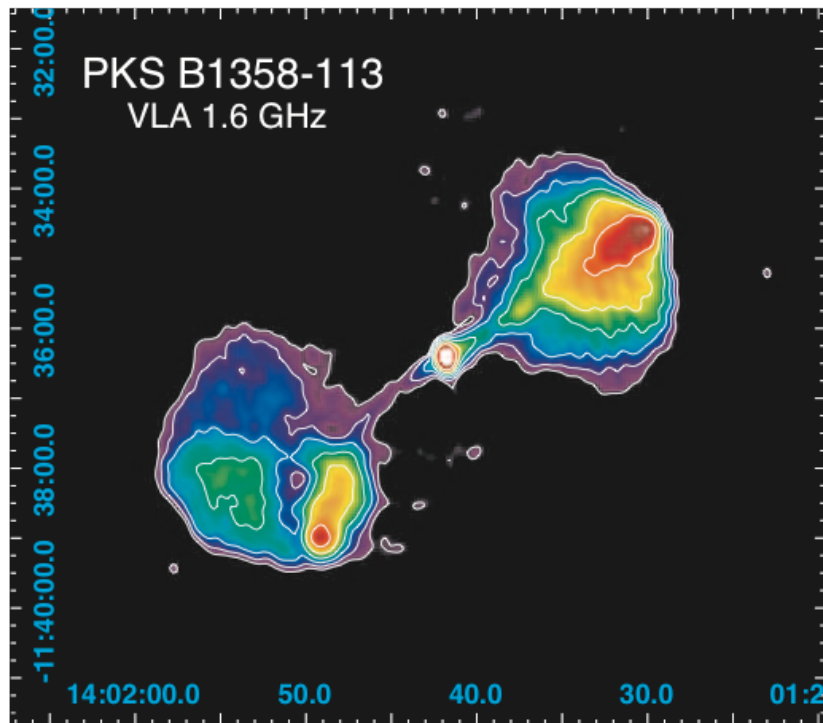
- FRI/FR II division based on the total radio power (Fanaroff & Riley 74), or radio power as a function of the optical luminosity of the host (Ledlow & Owen 96), is not really strict
- The often anticipated unification of FRI/FR II radio sources with LERGs/HERGs (Laing +94) is not really exact
- The common assumption that FR II nuclei are associated with standard Shakura-Sunyaev disks ($L_{\text{acc}}/L_{\text{Edd}} > 0.01$) while FR I with radiatively inefficient accretion flows ($L_{\text{acc}}/L_{\text{Edd}} < 0.01$), may in many cases be quite misleading

FRIIs at the centers of galaxy clusters

- Common at high redshifts, but then hardly accessible for detailed multiwavelength studies; at low redshifts only a few examples known (e.g., Cygnus A)
- We examined the NRAO VLA imaging survey of Abell clusters with $z < 0.25$ and $R \geq 0$ (Owen +92, Owen & Ledlow 97), and found only two FRIIs hosted by the BCGs (out of 400 systems): **PKS B1358-113 in A1836** ($z=0.0363$, $R=0$), and **4C+67.13 in A578** ($z=0.0866$, $R=0$).
- We have analyzed all the archival VLA data for the two selected systems, performed their optical spectroscopy using the William Herschel Telescope, and gathered the high-quality X-ray data with the XMM-Newton and Chandra satellites.

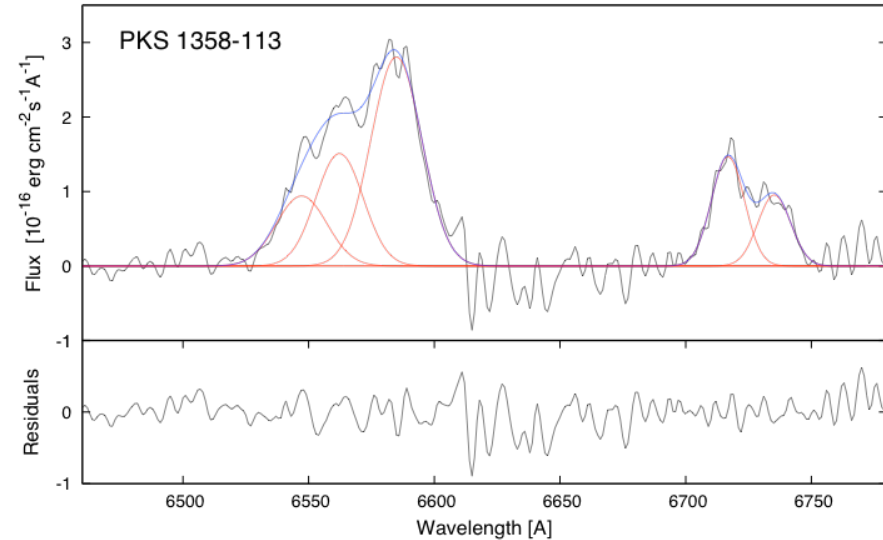
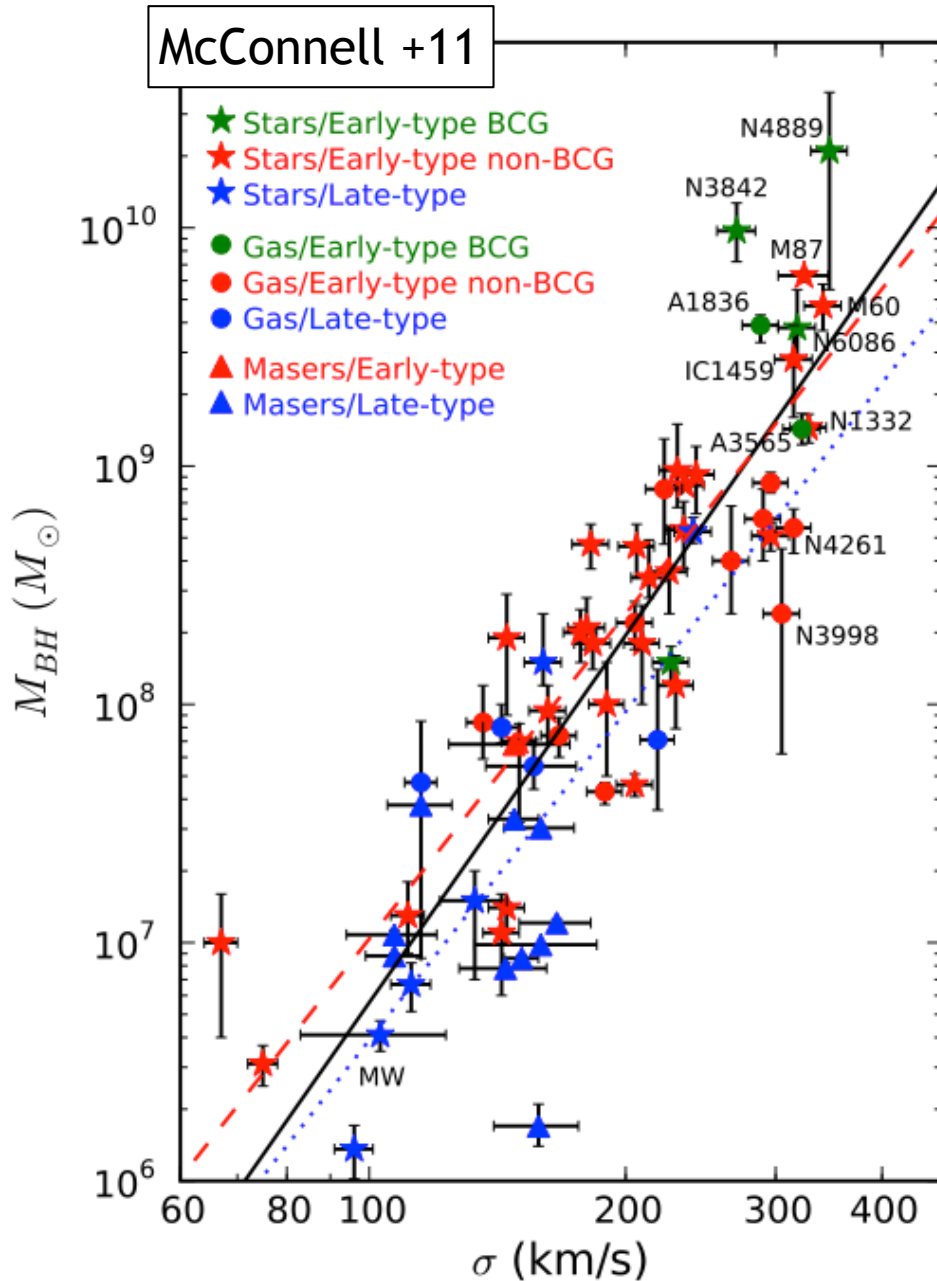
next slides: PKS B1358-113/A1836 case study (LS et al. 2014)

PKS B1358-113/A1836



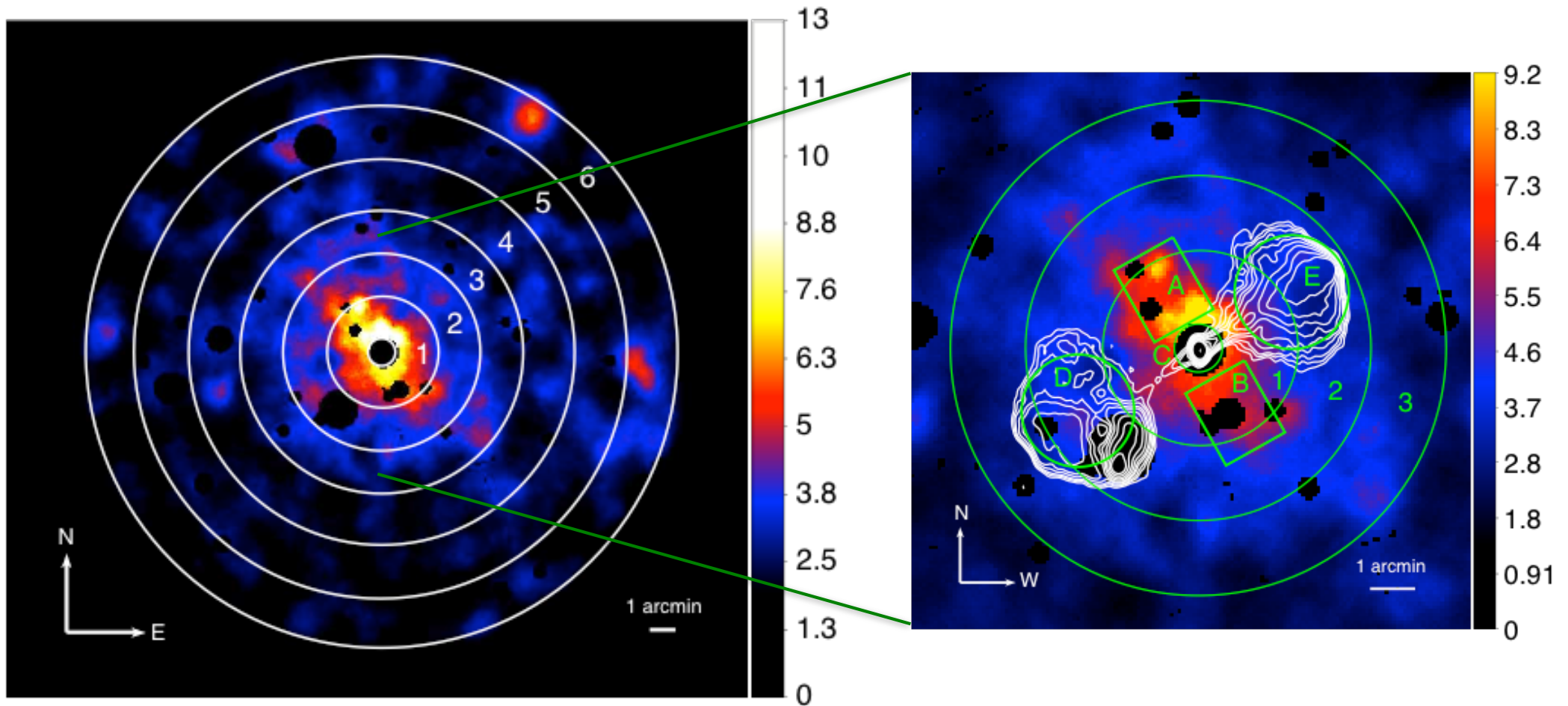
- Classical FR II radio morphology; radio power $L_{1.4\text{GHz}} = 8e40$ erg/s below the FRI/FR II division (host magnitude $M_R = -23.0$)
- Elliptical host with a mixture of 1 Gyr and 10 Gyr stellar populations, with no trace of young (<Gyr) stars (fit using the STRALIGHT code; Cid Fernandes +05)
- Velocity dispersion $\sigma = 295.0 \pm 6.0$ km/s

PKS B1358-113/A1836



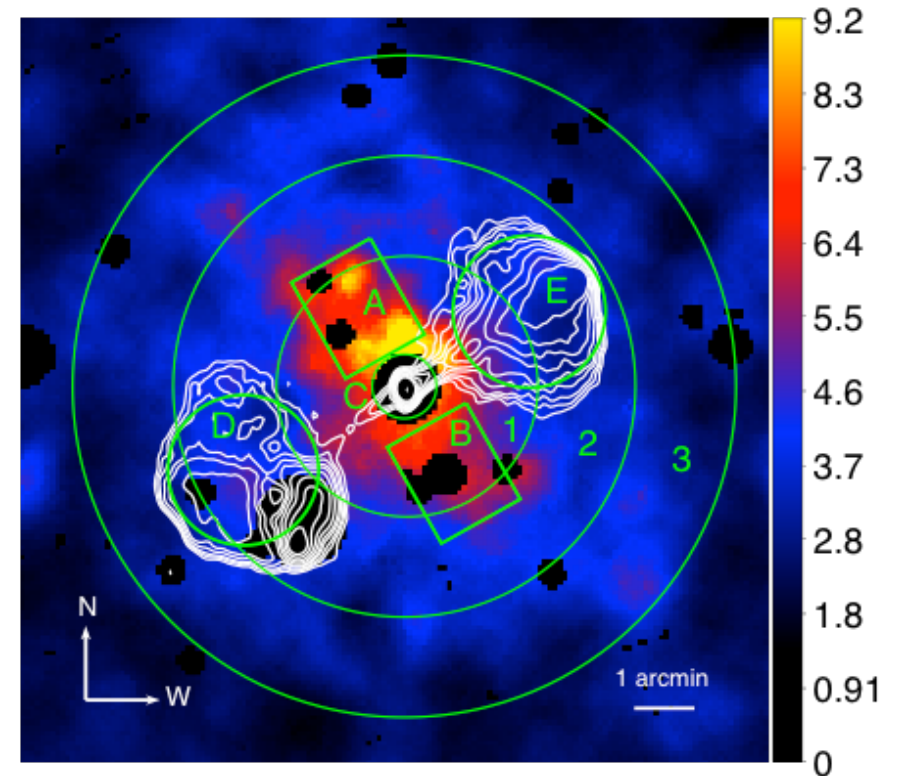
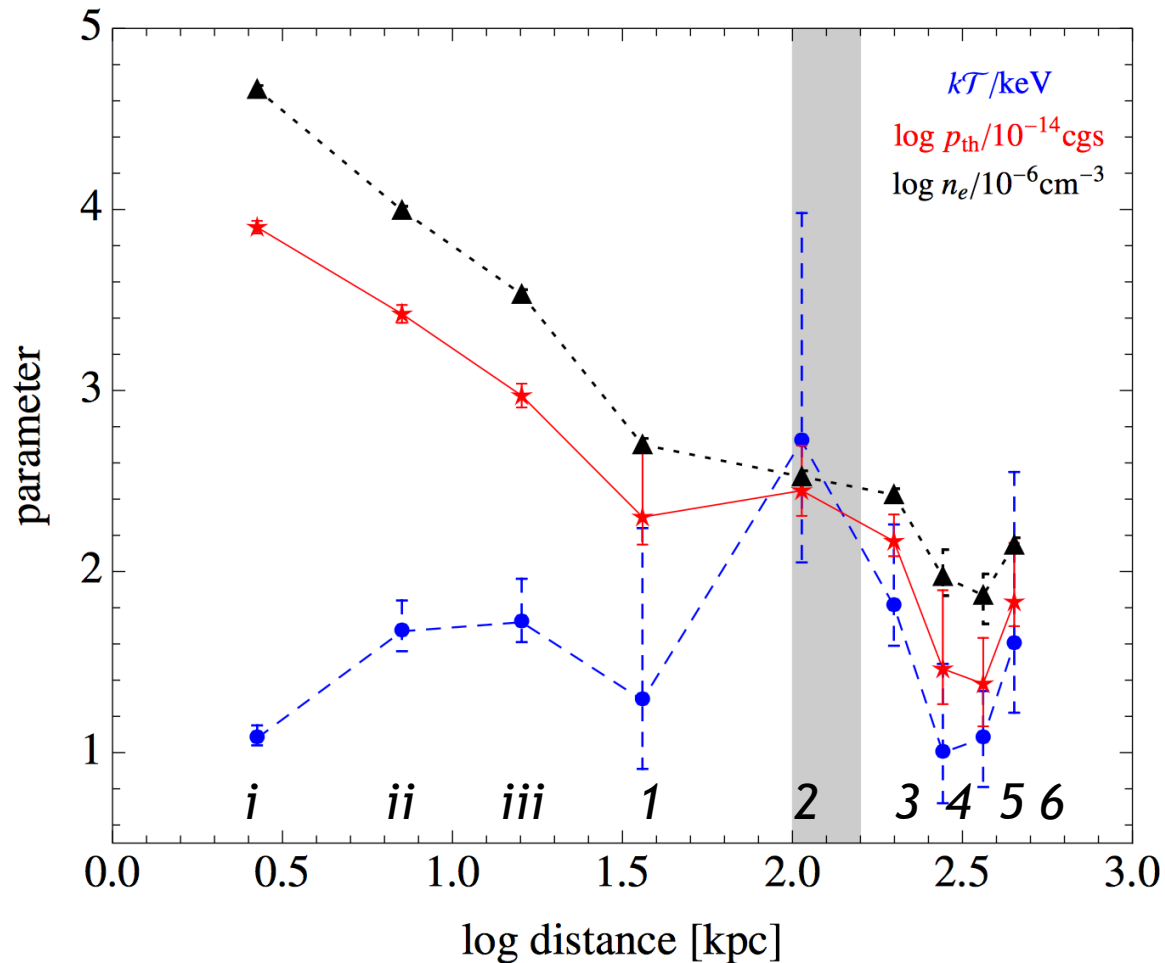
- BH mass $M_{BH} = 3.9e9 M_{\odot}$, one of the largest measured dynamically (McConnell +11), above the values implied by the $M_{BH}-\sigma$ and $M_{BH}-L_{bulge}$ scaling relations ($1e9 M_{\odot}$), and much above the “BH Fundamental Plane” ($0.6e9 M_{\odot}$)
- Line emission of the active nucleus of the LINER type, with $L_{H\alpha} = 1e40$ erg/s; consistent with our new Chandra observations indicating $L_{X,nuc} = 2e41$ erg/s
- The estimated accretion-related luminosity $L_{nuc} = 2e43$ erg/s implies a very low accretion rate in the source, $\lambda = L_{nuc}/L_{edd} \approx 4e-5$

PKS B1358-113/A1836



- Outer cluster emission ($32'' - 11'30''$ annuli 1-6; *XMM*): **ABS*APEC**
- Inner cluster emission ($2.5''-30''$ annuli *i-iii* within region C; *Chandra*): **ABS*APEC**
- Lobes (regions E and D; *XMM*): **ABS*PL**
- X-ray filament (regions A and B; *XMM*): **ABS*(PL+APEC)**
- Core ($<1.5''$ within region C; *Chandra*): **ABS*PL**

PKS B1358-113/A1836



- Total cluster luminosity $L_{0.3-10\text{keV}} \approx 4e42 \text{ erg/s}$ and the average cluster temperature $kT \approx 1\text{keV}$ consistent with the L_X - T relation derived for clusters and groups of galaxies (poor cluster)
- Gas temperature and density enhancements around the edges of the PKS B1358-113 radio structure revealed by the de-projected cluster profiles (but no obvious emissivity enhancements)
- Accretion radius ($r_A \sim 200\text{pc}$) still unresolved ($1'' = 0.71 \text{ kpc}$)

PKS B1358-113/A1836

- $\dot{M}_{\text{acc}} = \lambda (\eta_{\text{d}}/0.1)^{-1} \dot{M}_{\text{Edd}} \approx 2e-4 \dot{M}_{\text{Edd}} \approx 0.02 M_{\odot}/\text{yr}$ for the accretion disk radiative efficiency η_{d} at the level of a few percent (Sharma +07)
- Since we do not resolve the accretion radius in the system, we can estimate only a broad range of the Bondi accretion rate: $0.03 M_{\odot}/\text{yr} \ll \dot{M}_{\text{B}} \ll 2.5 M_{\odot}/\text{yr}$; this is much higher than the measured accretion rate \dot{M}_{acc}
- The fact that $\dot{M}_{\text{acc}} < \dot{M}_{\text{B}}$ is consistent with the expected mass-loss in radiatively inefficient accretion flows, $\dot{M}_{\text{acc}}(r < r_{\text{A}}) = (r/r_{\text{A}})^{\kappa} \dot{M}_{\text{B}}$ with $0 < \kappa < 1$ (Kuo +14, Nemmen & Tchekhovskoy 14)

PKS B1358-113/A1836

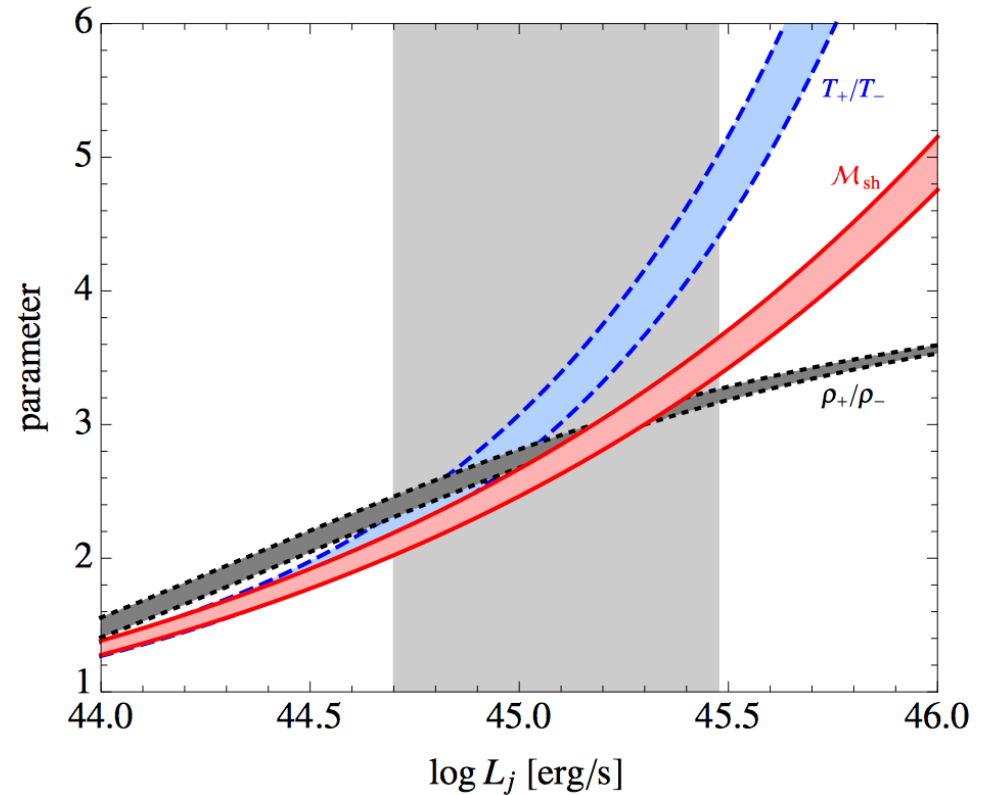
- $\dot{M}_{\text{acc}} = \lambda (\eta_d/0.1)^{-1} \dot{M}_{\text{Edd}} \approx 2e-4 \dot{M}_{\text{Edd}} \approx 0.02 M_{\odot}/\text{yr}$ for the accretion disk radiative efficiency η_d at the level of a few percent (Sharma +07)
- Since we do not resolve the accretion radius in the system, we can estimate only a broad range of the Bondi accretion rate: $0.03 M_{\odot}/\text{yr} \ll \dot{M}_B \ll 2.5 M_{\odot}/\text{yr}$; this is much higher than the measured accretion rate \dot{M}_{acc}
- The fact that $\dot{M}_{\text{acc}} < \dot{M}_B$ is consistent with the expected mass-loss in radiatively inefficient accretion flows, $\dot{M}_{\text{acc}}(r < r_A) = (r/r_A)^{\kappa} \dot{M}_B$ with $0 < \kappa < 1$ (Kuo +14, Nemmen & Tchekhovskoy 14)

Also

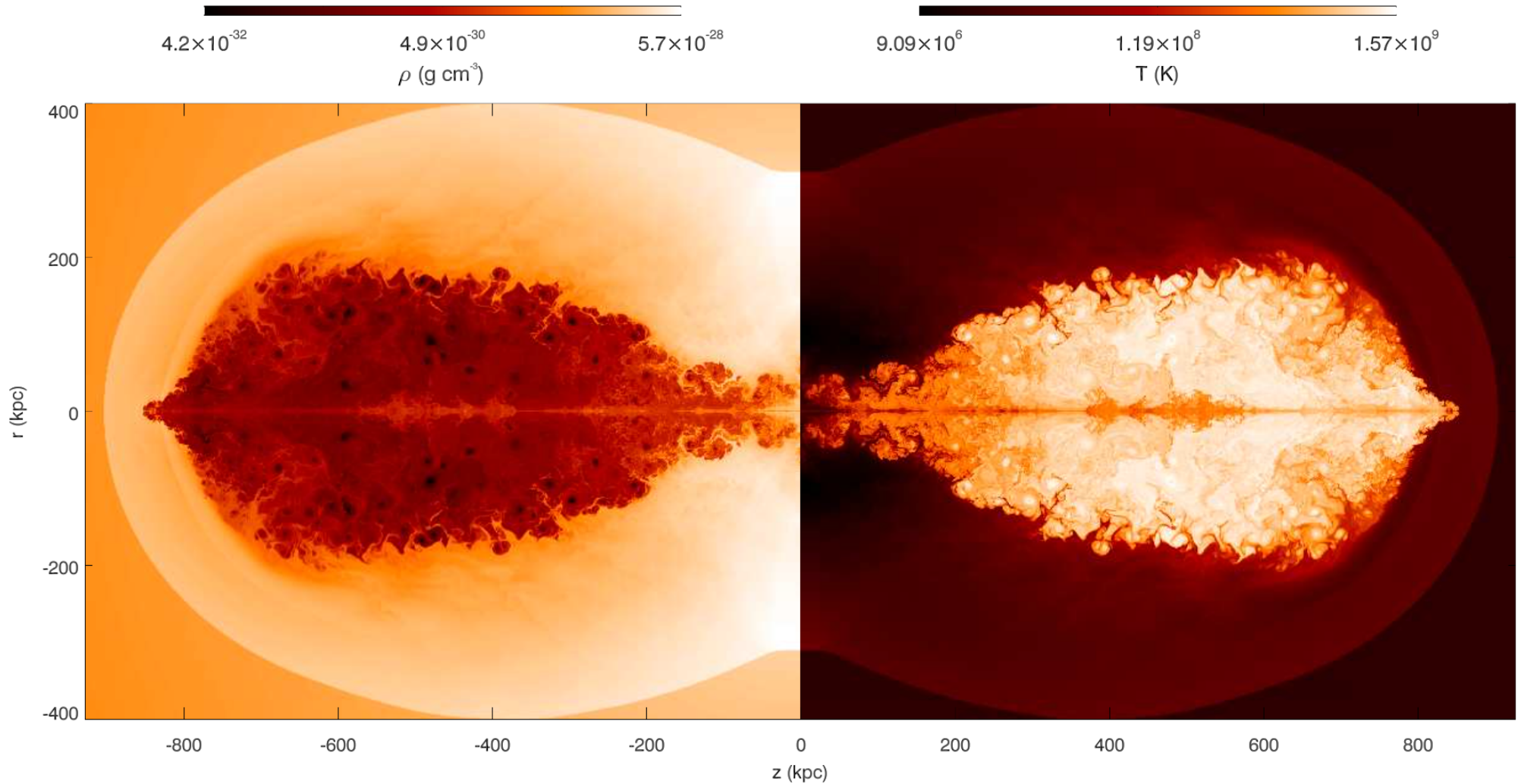
- Maximum jet kinetic luminosity $L_{\text{max}} = 3 \dot{M}_{\text{Edd}} c^2 \approx 3e45 \text{ erg/s}$ (McKinney +12, Tchekhovskoy +14)
- L_j - L_{rad} scaling relations derived for cluster radio galaxies (Birzan +08, Cavagnolo +10, O'Sullivan +11) return $L_j \sim (1-3)e44 \text{ erg/s}$; these relations are derived assuming sonic expansion of the lobes in the cluster atmosphere ($\tau_s \sim 300 \text{ Myr}$); and indeed for the analyzed system $L_{\text{cav}} = 4 p_{\text{th}} V_l / \tau_s \sim 1e44 \text{ erg/s}$
- Spectral analysis of the radio lobes at radio and X-ray frequencies indicates the lobes are over-pressured with respect to the surrounding medium, $p_l > p_{\text{th}}$, and relatively young, $\tau_j < 80 \text{ Myr} \ll \tau_s$; therefore $L_j > 4 p_l V_l / \tau_j > 5e44 \text{ erg/s}$

PKS B1358-113/A1836

- In the analyzed system the jet production efficiency is close to the maximum expected level: $L_j \approx (0.5-3) M_{\text{acc}}^* c^2 \approx (0.5-3)e45 \text{ erg/s}$
- The standard evolutionary model of FRILs applied to PKS B1358-113 confirms the supersonic expansion, with about half of the total jet energy, $E_{\text{tot}} = 2 L_j \tau_j \sim (2-8)e60 \text{ ergs}$, used for the shock-heating of the surrounding gas.
- The model-derived shock Mach number $M_{\text{sh}} \approx 2-4$ is consistent with the de-projected cluster profiles

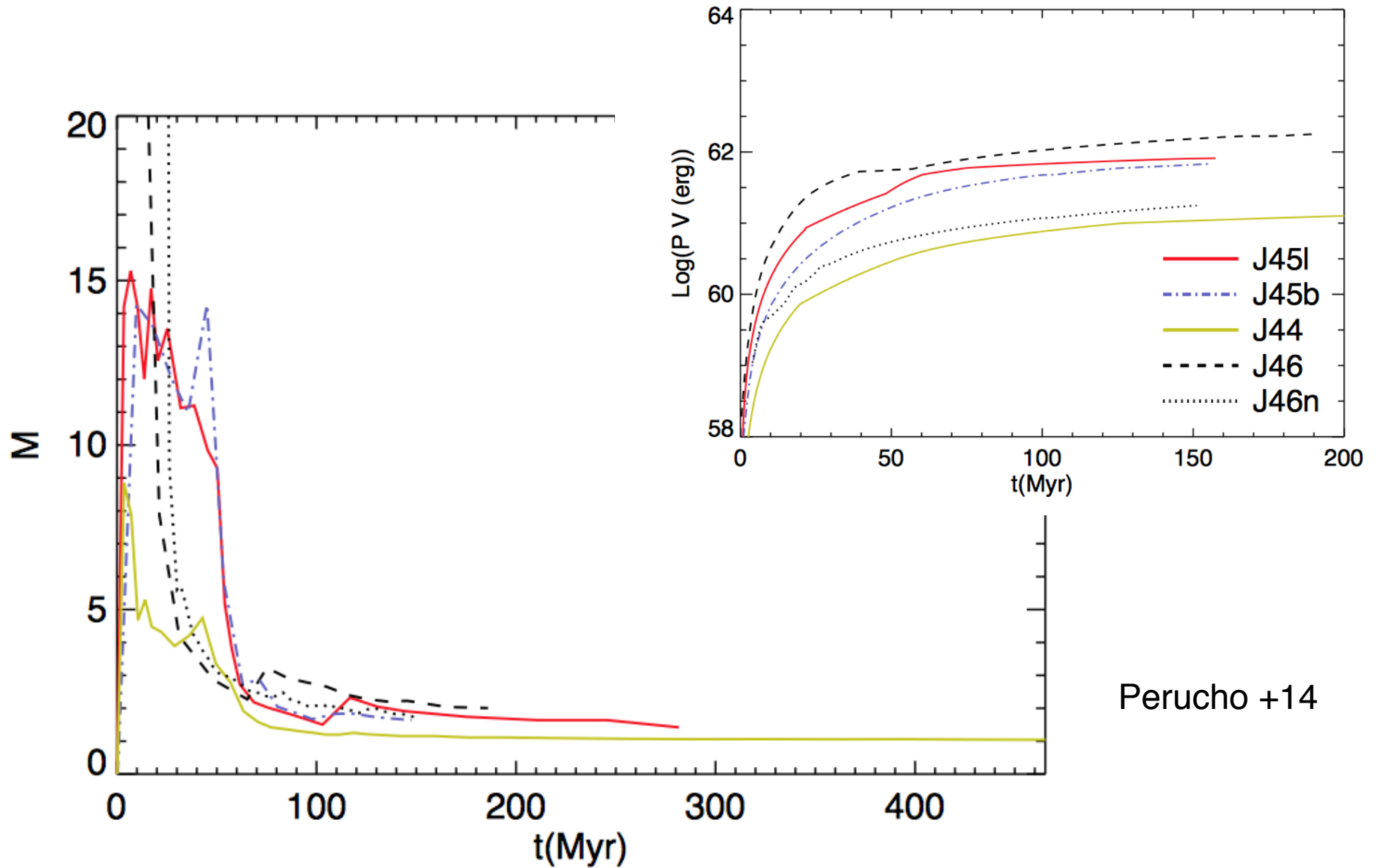


PKS B1358-113/A1836



Perucho +14: Density and temperature maps of models with $L_j = 1e46$ erg/s towards the end of the simulations, at $t \approx 180$ Myr.

PKS B1358-113/A1836



PKS B1358-113/A1836

- PKS B1358-113 is under-luminous in radio with respect to its FR II appearance
- BH mass much above the value implied by the BH fundamental plane
- Low accretion rate below the Bondi value, consistently with the expected mass-loss of RIAF
- Jet power higher than the cavity enthalpy divided by the sound-crossing timescale
- the L_j - L_{rad} or L_j - L_B scaling relations, often discussed for cluster radio galaxies, do not apply!
- Jet power close to maximum level allowed for a given accretion rate
- Efficient shock heating of the ambient medium by the expanding jet cocoon

PKS B1358-113/A1836

- PKS B1358-113 is under-luminous in radio with respect to its FR II appearance
- BH mass much above the value implied by the BH fundamental plane
- Low accretion rate below the Bondi value, consistently with the expected mass-loss of RIAF
- Jet power higher than the cavity enthalpy divided by the sound-crossing timescale
- the L_j - L_{rad} or L_j - L_B scaling relations, often discussed for cluster radio galaxies, do not apply!
- Jet power close to maximum level allowed for a given accretion rate
- Efficient shock heating of the ambient medium by the expanding jet cocoon

And in general

- Shocks surrounding radio lobes may be common and efficient in dissipating the jet kinetic energy (**just difficult to be detected for various reasons**)
- Need for detailed MWL studies of individual sources; to early to rely on various scaling relations derived for local weak sources (**especially when discussing the radio-mode feedback in high-z Universe!**)
- Jets seem to be produced with maximum allowed efficiency $L_j \sim L_{\text{acc}}$, depositing the bulk of the carried energy into their environments on 10s-100s of kpc scales

Conclusions

- Co-evolution of SMBHs and their host galaxies
- AGN feedback: fundamental component of semi-analytic models and hydrodynamic simulations of galaxy evolution
- so far only approximate “prescriptions” for the AGN feedback...
- AGN winds and jets: in principle enough energy, but how exactly coupled to the ISM/ICM?
- “radiative” vs. “mechanical” feedback
- jet energetics and duty cycle: crucial but still open questions
- observational evidence for dramatic interactions between AGN jets and their environment;
- jet-driven ionized, atomic, and molecular outflows in the ISM; quenching vs. inducing starformation?
- jet-inflated cavities in the ICM; shock heating?